Advanced botanical authentication of honey: Using an ultrasensitive electrochemical genosensor and RT-qPCR for the detection of *Castanea sativa*

Stephanie Morais [1,2], Eduarda Pereira [1-3], Mariana Ferreira [3,4], Marlene Santos [5], Sónia Soares [1], Ana L. Texeira [3], Valentina Domingues [1], Cristina Delerue-Matos [1] & M. Fátima Barroso [1*]

[1]REQUIMTE|LAQV, Instituto Superior de Engenharia do Porto, Instituto Politécnico do Porto, Porto, Portugal

[2] Departamento de Química, Faculdade de Ciências, Universidade do Porto, Portugal

[3] Molecular Oncology and Viral Pathology Group, Research Center of IPO Porto (CI-IPOP)/RISE@CI-IPOP (Health Research Network), Portuguese Oncology Institute of Porto (IPO Porto)/Porto Comprehensive Cancer Center (Porto.CCC), 4200-072 Porto, Portugal

[4] Research Department, LPCC-Portuguese League Against Cancer (NRNorte), 4200-172 Porto, Portugal;

[5] REQUIMTE|LAQV, Escola Superior de Saúde, Instituto Politécnico do Porto, Porto, Portugal

[6] ICBAS-School of Medicine & Biomedical Sciences, University of Porto, Porto, Portugal

Abstract:
Food fraud is a reoccurring issue for the food industry, with significant public health and economic implications. Honey, a natural ingredient prized for its sweetness and inherent nutritional profile and health benefits, is one of the most frequently adulterated foods found in the international market. This fraudulent act not only damages the reputation of the honey industry but also presents a hazard to the consumers' health. So, in this study, a disposable electrochemical genosensor was developed to detect *Castanea sativa* (chestnut tree) DNA in commercial honey samples. For this, a 103 bp *C. sativa* specific DNA-target oligonucleotide and its complementary probe were selected and designed. The genosensor methodology implied a sandwich hybridization format, for which the complementary sequence was cut into a 22 bp thiolated DNA-capture probe and an 81 bp fluorescein isothiocyanate-labelled DNA-signaling probe. Using chronoamperometric measurements, the enzymatic amplification of the electrochemical signal was obtained in a 0.03 to 1.00 nM concentration range, with a LOD and LOQ of 3.01 and 10.04 pM, respectively. The developed genosensor was able to detect the presence of the chestnut DNA in real chestnut plants and commercial honey samples. These results were then validated real-time quantitative PCR (RT-qPCR). In fact, conventional PCR coupled with gel electrophorese was not able to detect the presence of heather in honey. Therefore, electrochemical genosensors are a promising and cost-effective analytical tool to authenticate the botanical origin of honey, guaranteeing its safety, quality and authenticity.

Keywords: *Castanea sativa*, Food fraud, Electrochemical genosensor, Honey authentication, RT-qPCR.

1. Introduction

Food fraud is an emerging problem that concerns the food and beverage industries, quality control authorities and consumers alike, due to the potential health risks associated with the consumption of counterfeit products. These concerns are further amplified with the growing complexity of the global food supply chains and productions systems, which create new opportunities for fraudulent products to enter the market undetected [1,2]. To guarantee the quality of the ingredients the European Union (EU), for example, has implemented rigorous food safety regulations and regularly monitors the products introduced in the European market [2-4].

One sector under growing surveillance is the honey industry. Honey is a highly consumed natural product, appreciated worldwide because of its sweet taste, nutritional profile and health benefits, like its low glycemic index [2,5,6]. However, these characteristics are not uniform and vary contingent on factors like the beekeeping practices, local climate and geography and the plant species from which the nectar was harvested by the bees [7,8]. A honey's botanical origin, for instance, is one of the most determining factors in the final composition and beneficial health properties of the product. Consequently, honey can be classified as monofloral (if the honey originates predominantly from a specific plant source) or multifloral (if derived from various plant sources) [6]. Except the honey from over-represented (like *Castanea sativa*, *Echium plantagineum*, *Eucalyptus globulus*, *Helianthus annuus,* ...) or under-represented taxa (e.g., *Arbutus unedo*, *Lavandula stoechas*, *Citrus sinensis*, *Thymus vulgaris,* …), honey is usually considered monofloral if the total pollen content of that predominant plant is more than 45% [7,9].

The interest in monofloral honeys lays in their unique sensory characteristics at are tied to the floral source and hold greater commercial value than multifloral honeys [7-9]. Thus, monofloral honey with products from specific regions are eligible for Protected Designation of Origin (PDO) or Protected Geographical Indication (PGI) status. These designations are linked to the local environmental and human aspects, which impart specific qualities to honey by enhancing their distinctive flavor profiles, therapeutic properties and perceived higher quality, and subsequently elevating the market value of monofloral PDO and PGI honeys [7,10].

As of 2023, there were 3,000 PDO and PGI honeys registered in the EU, with Portugal holding the highest number (9 PDO honeys), followed by Spain (5 PDO) and France (3 PDO and 2 PDI) [11,12]. This makes them a prime target for adulteration, particularly through mislabeling of its botanical and geographical origin or mixing with lower-quality substances. So, the increase in consumer demand for natural and health-promoting food products has further elevated their economic importance and susceptibility to fraud [6]. For instance, in 2022, the EU honey production met only 60% of internal demand, making the bloc heavily reliant on imports. However, recent investigations have revealed widespread irregularities, particularly among imported honeys. Around 46% of honey samples imported from non-EU countries were suspected of violating the Honey Directive [13].

One of the earliest approaches to detect fraudulent honeys involves examining its texture, structure and chemical makeup. Nevertheless, assessing the physical and chemical properties of honey typically require detailed knowledge of authentic honey characteristics and are effective only for specific varieties. Complications arise due to the vast plant diversity across different regions and seasonal fluctuations in pollen type, which hinder accurate pollen identification [2,6,7,14]. Still melissopalynology remains one of the most widely used techniques for verifying honey's botanical and, to some extent, geographical origin. While effective, this method is labor-intensive, time-consuming, and demands expert knowledge of pollen morphology [6,14]. As the number of samples increases, so does the need for labor, along with the demand for advanced skills and precision in conducting the tests. Inadequate care during analysis can lead to inaccurate results. Thanks to these limitations, there is a growing need for efficient, reliable and broadly applicable techniques to distinguish honeys of different botanical origins [6].

In this study, the botanical DNA of *Castanea sativa* (a prominent species in the north of Portugal was detected by an electrochemical genosensor specifically designed to register the sandwich format DNA hybridization reaction between two *C. sativa* complementary probes in real samples DNA [15]. Analysing public database platforms, a 103 base-pair DNA-target probe capable of unequivocally detecting the pollen from *C. sativa* was selected and designed. The complementary probe to the DNA-target oligonucleotide sequence was then cut into a 22 base-pair thiolated DNA-

capture probe and an 81 base-pair fluorescein isothiocyanate-labelled DNA-signaling probe. To increase the hybridization reaction, a self-assembled monolayer formed from mixing the DNA-capture probe with mercaptohexanol was employed (**Figure 1**).

Using chronoamperometry, the enzymatic amplification of the electrochemical signal was achieved with a concentration range of 0.03 to 1.00 nM. The genomic DNA from certified *C. sativa* plants was extracted and the targeted region amplified by conventional PCR. Then, the amplified material was applied to the developed electrochemical genosensor and dilutions compared to the calibration curve from the synthetic probes. The genomic *C. sativa* DNA registered current intensities in the same range as the synthetic probes, especially in the lower concentrations. Conventional PCR and real-time quantitative PCR (RT-qPCR) analysis were also later employed to validate the attained chronoamperometric responses.

The validation test performed by conventional PCR revealed little to no amplification of extracted DNA products from the plant and honey samples. However, the RT-qPCR analysis produced melting curve with single and well-defined peaks for all reactions, thus confirming the specificity of the amplified RT-qPCR products. These results not only prove that the designed primers are functional and suitable for the detection of their respective targets but also the effectiveness and sensitivity of the developed genosensor. Hence, electrochemical genosensors are a more sensitive and cost-effective tool to facilitate the authentication process of honey samples and, hopefully, promote food safety and control.

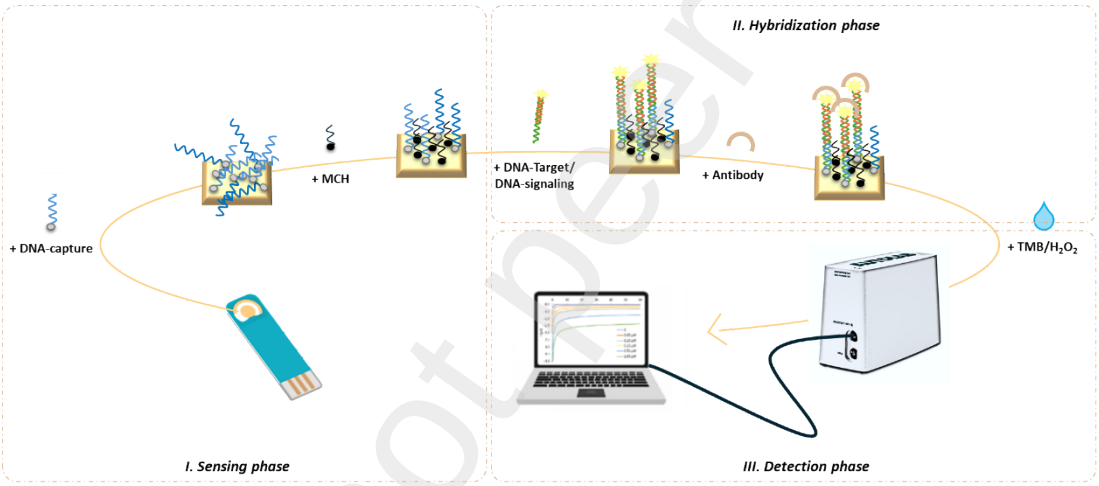

Figure 1. General design of the electrochemical genosensor.

2. Materials and methods

2.1. Reagents and solutions

3,3′,5,5’ tetramethylbenzidine (TMB), 20x sodium phosphate-EDTA (200 mM sodium phosphate, 3 M NaCl, 20 mM EDTA) pH 7.4 solution (20× SSPE) and 6-mercapto-1-hexanol (MCH) were obtained from Sigma Aldrich. The SSPE (20x) buffer was diluted to SSPE (2x) with Milli-Q ultrapure water obtained from a Millipore purification system. Absolute ethanol, anti-fluorescein-peroxidase (anti-FITC-POD) antibodies and Casein phosphate-buffer saline (PBS) was acquired from Carlo, Roche and Thermo Scientific, respectively. All the reagents were of analytical grade, so no purification was required.

For the pre-treatment of the chestnut plant and commercial honey samples, the Easy Pure Food and Fodder Genomic DNA kit from TransGen Biotech Co., Ltd. (Beijing, China) was utilized. This kit aided in the separation of the plant DNA from the other cellular components in the samples. Furthermore, a Taq Master Mix (2x), an optimized and ready-to-use PCR mixture with Taq DNA Polymerase, 2 mM of magnesium chloride ($MgCl_2$), deoxynucleotide triphosphates (dNTPs) and PCR water (acquired from Bioron) were used for the amplification of the genetic material by conventional PCR.

To validate the effectiveness of the amplification process, Agarose (GRS Agarose LE) and the 20x SGTB buffer, diluted to SGTB 2x, both from GRISP Research Solutions, were utilized to produce the electrophoresis gel. Likewise, a 25x SYBR Green I Nucleic Acid Gel Stain solution (Invitrogen, ThermoFisher Scientific) with the Absolute Q DNA Digital PCR Master Mix (5x) and nuclease-free water (Applied Biosystems®) were used to perform and visualize the amplifications for the RT-qPCR and digital PCR assays.

2.2. Apparatus and electrodes

To extract the DNA from the chestnut plants an iron mortar and pestle were used to shred the leaves. Moreover, an ultrasonic probe (Ultrasonic Processor/Sonicator, CV334 Converter, Sonics®, Vibra Cell™) was used to homogenize and help separate the cell components from the genomic DNA. Then, the amplification of the targeted DNA region was carried out using the conventional PCR technique in a two-unit GeneTouch thermocycler from Bioer.

A microplate reader (Synergy HT, BioteK) was utilized to quantify the extracted genomic DNA, and the results of the genomic DNA amplification were visualized using a Gel Doc XR Imaging System (Bio-Rad). A Fisherbrand PCR thermalblock was also utilized to heat the oligonucleotide sequences and molecular biology reagents.

The electrochemical genosensors were constructed using low temperature screen-printed gold electrodes (SPGE, C223BT DropSens, from ΩMetrohm), as the transductor. These SPGE are composed of a gold working electrode (Ø 1.60 mm), a silver pseudo-reference electrode and a gold counter electrode, deposited over a flat ceramic chip.

An Autolab electrochemical potentiostat (PGSTAT101, ΩMetrohm) equipped with the NOVA 1.10.1 software was used to measure all the chronoamperometric responses. Chronoamperograms were recorded at − 0.10 V for 60 s. Meanwhile, cyclic voltammetry (CV) and electrochemical impedance spectroscopy (EIS) measurements were carried out on a PalmSens4 (Bi)Potentiostat/Galvanostat/Impedance Analyzer (PalmSens) equipped with the PSTrace 5.11 software. CVs measurements were carried out from − 0.20 V to + 0.60 V for two cycles with a 2.50 mM $[Fe(CN)6]^{-3/-4}$ solution prepared in KCl.

2.3. Oligonucleotides

The designed oligonucleotide sequences (**Table 1**) used in this experiment were purchased from Eurogentec as a lyophilized salt. Every oligonucleotide stock solution was resuspended to 100 nM with Milli-Q ultrapure water and stored at − 20°C. Meanwhile, working oligonucleotides were prepared daily by diluting the required concentration in the 2x SSPE buffer.

The design of the primers was carried out using Primer-Blast (NCBI) [16] and the selected sequences purchased from Eurogentec.

Table 1. Oligonucleotide sequences designed for *Castanea sativa*.

Oligonucleotide	Sequence 5' → 3'	Base pairs (bp)
DNA- capture	**SH**-ATC AGA GGA TGA GTG GGA CCA C	22
DNA-signalling	CTA TAA AAT TTC ATG ACT CTA TGA ATT GTG TGT GTG TGT GTG TGT GTG GGG AGA TTT CCA TTG ATA TGG CGG GCT GTC TTC-**FAM**	81
DNA-target	GAA GAC AGC CCG CCA TAT CAA TGG AAA TCT CCC CAC ACA CAC ACA CAC ACA CAC AAT TCA TAG AGT CAT GAA ATT TTA TAG GTG GTC CCA CTC ATC CTC TGA	103
Primer Forward	GAA GAC AGC CCG CCA TAT CA	20
Primer Reverse	ATC AGA GGA TGA GTG GGA CC	20

SH - thiol group; **FAM** - fluorescein.

2.4. Characterization of the screen-printed gold electrode surface by CV and EIS

To characterize the surface of the working electrode during the "Electrochemical genosensor design" step, cyclic voltammetry (CV) and electrochemical impedance spectroscopy (EIS) was performed in 2.50 mM $[Fe(CN)_6]^{3-/4-}$ prepared in KCl.

2.5. Electrochemical genosensor design

Four steps were applied for the construction of the electrochemical genosensor: a pretreatment; a sensing phase, the sandwich hybridization reaction and the electrochemical detection. The pretreatment step is a surface cleaning process that occurs before the immobilization of the oligonucleotides. So, before use, all electrodes are washed with ethanol and ultrapure water and then dried under a nitrogen flow.

To guarantee the linear orientation of the probes, a self-assembled monolayer (SAM) interface between the DNA-capture probes and the MCH spacer was arranged (sensing phase). For this, 3 µL of the chestnut flower DNA-capture probe was immobilized onto the surface of the SPGEs' working electrodes and stored in a humified Petri dish overnight. On the next day, the modified electrodes were rinsed with the SSPE 2x buffer (400 µL), in order to remove the weakly attached DNA-capture probes. Afterwards, 3 µL of MCH was applied to the working electrode's surface.

The sandwich format hybridization assay proceeded in a two-step hybridization: the homogeneous hybridization takes place when the DNA-signaling probe binds to the DNA target in the buffer solution, for 30 min. Then, the resulting solution was added to the modified electrode which leads to the binding of the semi-complementary DNA-target/DNA-signaling probes to the immobilized DNA-capture probes – the heterogeneous hybridization.

After an hour, the electrodes were rinsed to remove any nonspecific adsorbed sequences. The sandwich hybridization format enhances assay selectivity by facilitating two distinct hybridization events: the homogenous hybridization between the target and the signaling probe and the subsequent binding of an anti-fluorescein antibody labeled with a horseradish enzyme to the fluorescein-labeled signaling probe. To detect the electrochemical signal, POD enzymes in a PBS buffer solution were added onto the electrode's surface. The electrode was rinsed again after a brief period of time.

Finally, the genosensor was connected to the potentiostat and 40 µL of the TMB/H_2O_2 substrate was applied over all three electrodes for 1 min. The detection of the enzymatically oxidized product was conducted by chronoamperometry at − 0.1 V, for 60 s. The measurements are performed in triplicate for accuracy.

2.6. Botanical and honey samples

2.6.1. *Castanea sativa* plants

Plant samples from *C. sativa* (European chestnut tree) were obtained from the Natural Park of Montesinho in Bragança, Portugal. Liquid nitrogen was used to dry the plants, and their genomic DNA extracted by mechanically shredding the plants with an iron mortar. *Erica arborea* (the white heather tree flower) was used as a negative control.

2.6.2. Honey samples

Twelve commercial honey samples (legend H1 to H12), purchased from local Portuguese markets, were also applied to the developed sensor in order to validate the sensor's selectivity. These honeys stem from different regions of continental Portugal.

2.6.3. Pre-treatment of the honey samples and the plant specimens

Two distinct protocols were applied for the isolation of the pollen from the honey samples. The first was based on the CTAB DNA extraction protocol Doyle & Doyle, 1987 [17] while the second was adapted from a protocol proposed by Soares et al., 2015 [18]. Briefly, for the CTAB procedure, 2 mL of the CTAB buffer was added to the extracted DNA samples, followed by 4 µL of β-mercaptoetanol. Each sample was then vortexed for 10 s. Afterwards the samples were incubated at 65 ± 2ºC, for 30 min, and centrifuged for 5 min at 6,000 rpm. The resulting supernatant (approximately 1 mL) was then transferred to a new eppendorf, where 1 mL of a chloroform/isoamyl alcohol mix (in a 24:1 ratio) was combined. Next, the material was vortex until

an emulsion formed and centrifuged at 15,000 rpm for 5 min. Subsequently, the supernatant was transferred to a new eppendorf and 0.60x of very cold isopropanol was added to each sample. The samples were then mixed by inversion and incubated at − 20ºC during 30 min. After that, all samples were centrifuged at 14,000 rpm for 20 min and the obtained supernatant discarded. Following this, 700 µL of 70% ethanol were added to the mix and the samples were centrifuged at 14,000 rpm for 10 min. After the centrifugation the supernatant was discarded, only preserving the *pellet*. This step was repeated two times (2x) before leaving the samples open overnight to finish evaporating any remaining ethanol. Finally, 100 µL of ultrapure water was added and stored at – 20ºC until use.

As for the Soares et al., procedure, 10 g of each honey sample were transferred to 50 mL Falcon tubes and frozen at – 80ºC overnight. Afterwards, 45 mL of warm water (± 45ºC) was added to each Falcon and vortexed until the honey dissolved in the water. Once dissolved, each honey sample was agitated by an ultrasonic probe with an amplitude of 20% for 3 min and subsequently left in a 45ºC water bath for 60 min. The sample was then centrifuged at 10,000 xg for 20 min. The resulting supernatant was discarded, and its *pellet* resuspended in 2 mL of deionized water. Following two centrifugations at 17,000 xg for 10 min where, in both cases, the supernatant was discarded. In the end, the remaining *pellet* was preserved and stored at – 20ºC until use.

2.7. Molecular biology techniques

Conventional PCR and real-time PCR (RT-qPCR) were used to validate the results registered by the developed electrochemical genosensor. The *C. sativa* primers were utilized in both PCR methods. However, before use, the plant and honey samples were submitted to a pre-treatment and extraction process. The pre-treatment and extraction processes were different for both biological samples.

2.7.1. Extraction of genomic pollen DNA from honey samples and plant specimens

The isolation of the genomic DNA from the plant specimen (*C. sativa*) and the twelve honey samples were carried out according to the manufacturer's recommendation from the Easy Pure Food and Fodder Genomic commercial DNA kit protocol.

2.7.2. Conventional PCR

The protocol established by Bioron was employed for the preparation of the PCR mixtures, and the GeneTouch thermocycler from Bioer was used for the amplification of the samples.

2.7.3. Real time quantitative PCR

Relative quantification of the target DNA sequence was performed by RT-qPCR using the StepOne™ PCR System (Applied Biosystems®). Data analysis was carried out with StepOne™ Software v2.3 (Applied Biosystems®). For the reactions, the SYBR Green Absolute Q DNA Digital PCR Master Mix (4x) was used, combining 25X SYBR Green I solution with the Absolute Q DNA Digital PCR Master Mix (5x), nuclease-free water and 2 µl of target DNA, in a final reaction volume of 10 µl.

For the *C. sativa* DNA sequence amplification, specific primers were used: Forward [5´-GAA-GAC-AGC-CCG-CCA-TAT-CA-3´] and Reverse [5´-ATC-AGA-GGA-TGA-GTG-GGA-CC-3´], both at a final concentration of 200 µM. The thermal cycling program consisted of an initial denaturation at 95°C for 20 s, followed by 40 cycles of denaturation at 95°C for 3 s and annealing/extension at 62°C for 30 s. The corresponding melting curve revealed a melting temperature of 79.12°C.

To validate amplification performance, efficiency curves were generated for all primer sets, with efficiencies consistently above 90%. Negative controls were included in each run.

3. Results and discussion

3.1. Selection of the DNA probes

For the construction of the chestnut flower-specific electrochemical genosensor, a 103 base pair synthetic DNA-target sequence capable of detecting *C. sativa* pollen DNA present in real honey samples was selected and designed (**Table 1**). The complementary sequence to the DNA-target was in silico cleaved in two smaller DNA fragments: a 22 bp DNA-capture and an 81 bp DNA-signaling probe. The capture and signaling probes were also designed to minimize the formation of secondary structures, since on a planar surface (such as the gold electrode) strong secondary structures may hinder the hybridization process.

3.2. Characterization of the electrode surface

CVs and EIS (**Figure 2**) were utilized to analyze the electrochemical behavior of the SPGEs' surface along the various modification steps (DNA-capture, MCH, dsDNA hybrid) when compared to the bare surface electrode with 2.50 nM $[Fe(CN)_6]^{3-/4-}$ in KCl. The resulting CVs and EIS Nyquist plots are represented in **Figure 2**.

From the CVs responses (**Figure 2A**) it is visible that the various analytical optimizations led to an alteration to the electrode's surface, indicating the effectiveness of the hybridization process. Compared to the bare electrode, the other modifications generally resulted in a reduction of the $[Fe(CN)_6]^{3-/4-}$ redox current intensity and increase peaks potentials. The biggest difference between the electrodes was observed between the bare SPGE and the Au/DNA-capture electrode; the bare SPGE presented an oxidation peak intensity of 20.46 µA with an oxidation potential of 0.19 V and a reduction peak intensity of 0.05 µA with a reduction potential of – 20.15 V, meanwhile the Au/DNA-capture electrode registered an oxidation peak intensity and potential of, respectively, 8.67 µA at 0.35 V and a reduction peak intensity and potential of – 0.07 µA at – 8.35 V.

For the EIS analysis, charge-transfer resistance (Rct) was the chosen parameter. This resistance was calculated based on the Nyquist plots (**Figure 2B**) obtained from the EIS study. According to the literature, the more blocked the electrode surface the higher the Rct value since the area where the hybridization reaction can occur will be smaller [19,20].

As observed in **Figure 2B**, the lowest Rct value corresponds to the bare electrode (Rct = 111.65 Ω), meanwhile the highest Rct (21630.29 Ω) was obtained after the addition of the DNA-capture probes. The increased concentration of DNA-capture (1.00 µM) immobilized onto the working electrode's surface exponentially increased the Rct value, thus blocking the biosensor's surface. However, and contrary to the expected, the addition of MCH reduced the Rct to 975.36 Ω, thus decreasing the surface blockage [21]. This result can be explained by the interaction between the DNA-capture probes with MCH; MCH helps space and linearly orientate the DNA-capture oligonucleotides by creating openings in the electrode's surface that facilitate the hybridization reaction between the previously immobilized sequences and the DNA-target probes [22-24]. Therefore, this Rct value confirms that the available surface area increased after the addition of MCH.

Afterwards, to determine the difference between the bare and dsDNA hybrid response, the Rct value of the two assays were also analyzed. Unexpectedly, the electrodes immobilized with the dsDNA hybrid also registered a low Rct value (443.11 Ω). This response was unexpected but within the predictable range since, after adding MCH and rinsing the electrode's surface, any poorly attached probes were removed [19,25].

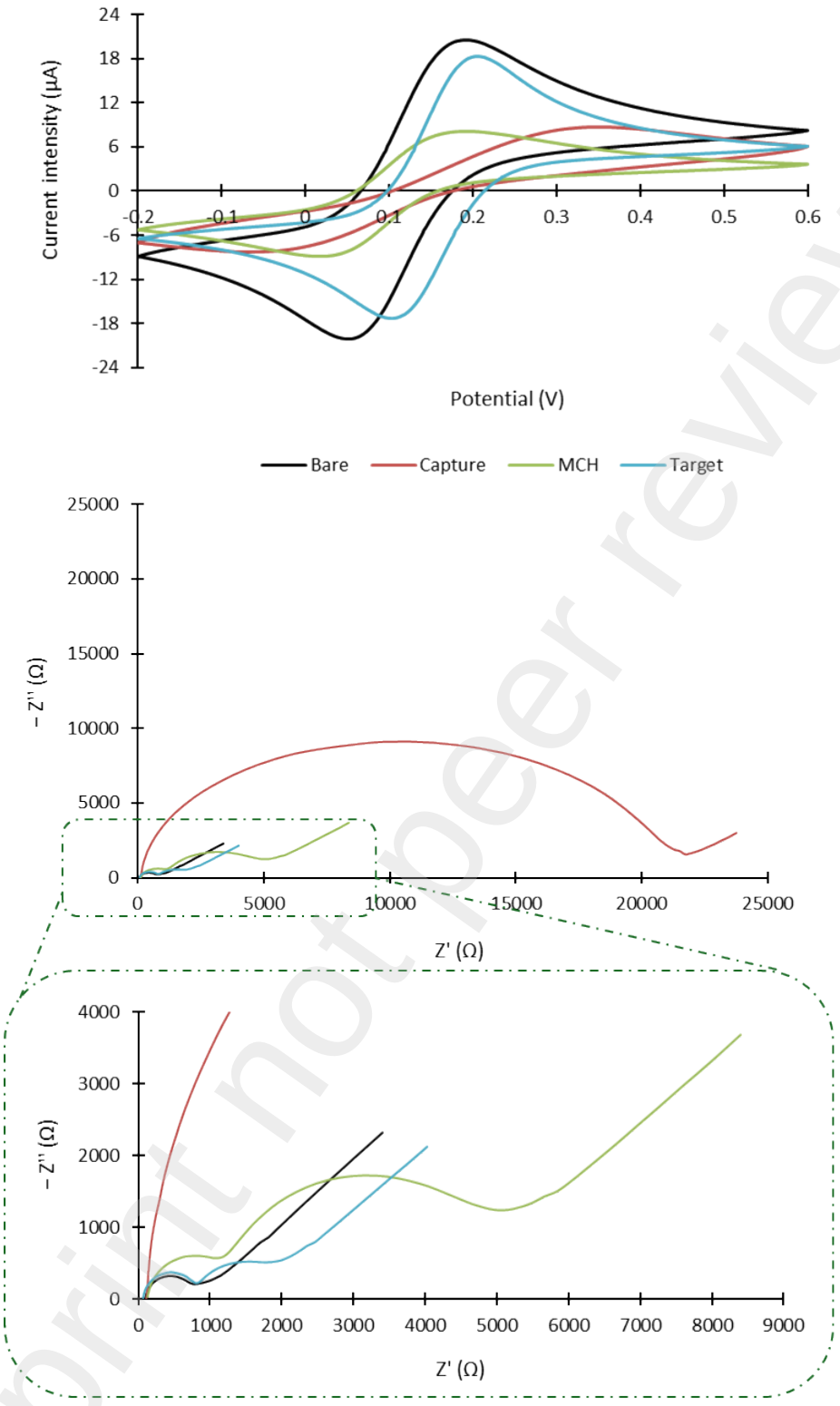

Figure 2. Characterization of the bare gold (Au) (black), DNA-capture modified (Au/DNA-capture, red), mercaptohexanol modified (Au/DNA-capture/MCH, light green) and doble stranded (dsDNA) hybrid (Au/DNA-capture/MCH/DNA-target/DNA-signaling, light blue) electrode surface by cyclic voltammograms (A) and Nyquist plots resulting from electrochemical impedance spectroscopy (B). All measurements were recorded at 2.50 mM $[Fe(CN)_6]^{-3/-4}$ prepared in KCl.

3.3. Optimization of the experimental parameters

The main selection criteria for the optimization of the experimental variables involved in the DNA-based sensor's design is the largest ratio between the chronoamperometric signals measured at

– 0.10 V (vs. the silver pseudo-reference electrode) for 0.00 nM (blank, B) and 1.00 nM of synthetic DNA-target concentration (signal, S), i.e., the signal-to-blank (S/B) ratio. The highest cathodic electrochemical current intensity value (I) was only applied when similar S/B ratios were obtained. The electrical current used for analytical purposes corresponds to the average of the currents obtained in the last 10 s of the measurement.

3.3.1. Optimizations for the sensing phase

The experimental parameters related to the sensing phase, namely the concentration of the DNA-capture, as well as the concentration and the incubation time of MCH, were the first optimizations performed for the development of this sensor (**Figure 3**). For the DNA-capture probe concentration, three concentrations ranging from 0.25 to 1.00 µM were immobilized onto the SPGE working electrode in order to determine its influence on the intensity of the electrochemical currents (**Figure 3A**).

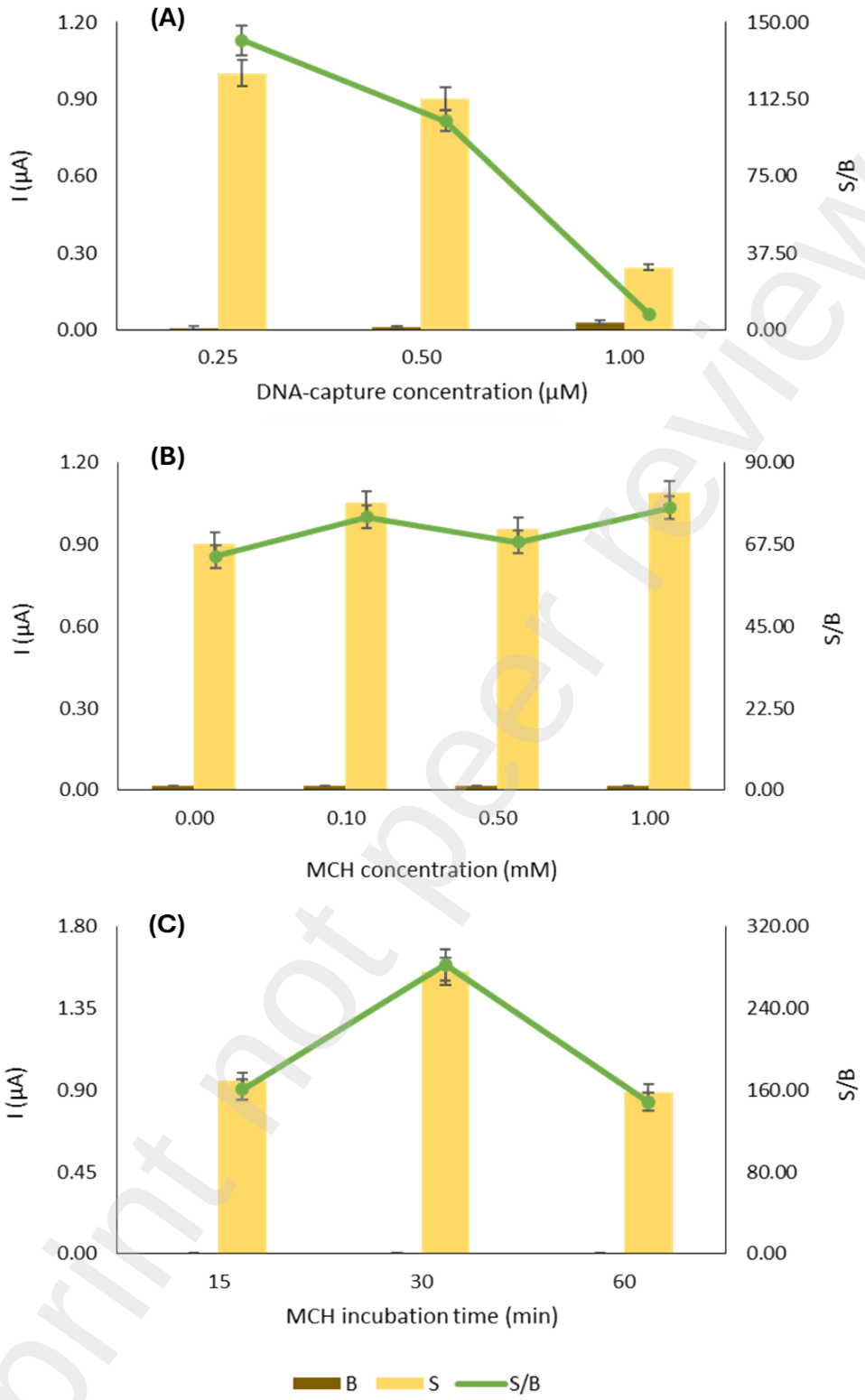

Figure 3. Chronoamperometric responses acquired when optimizing the concentration of the DNA-capture probe (A), and the concentration (B) and incubation time of MCH (C). Blank values (B) represented in dark brown, signal (S) in light yellow and the corresponding S/B ratio in green. Error bars estimate the standard deviation of three replicates.

As observed in **Figure 3A**, increasing the probes' concentration leads to a reduction in the current intensity. As such, the electrodes with the highest S/B ratio value (S/B = 141.09), as well as the highest current intensity (I = 1.00 µA), were those immobilized with the DNA-capture of 0.25 µM, followed by the 0.50 µM concentration with a S/B ratio and intensity of 101.90 and 0.90 µA, respectively. Thus, the worst response was obtained with the highest concentration of the DNA-

capture sequences were immobilized on the working electrode's surface (S/B = 8.06 and I = 0.24 μA).

Based on literature, better analytical signals can be attained if the if the oligonucleotide sequences, on gold platforms, are linearly oriented. Hence, when in contact with larger molecules, MCH (a thiol with a six-carbon chain) can act as a molecular spacer minimizing the adsorption of nonspecific biomolecules and easing the permeability of other molecules. Therefore, the addition of MCH to the electrochemical genosensor is an important step since it helps the DNA-captures probes to linearly orientate themselves as self-assembled monolayers (SAMs). Thus, the subsequent optimizations were the concentration and incubation period of MCH (**Figure 3B** and **3C**, respectively).

So, firstly, under the new analytical conditions (0.25 μM of the DNA-capture probe and 1.00 nM of DNA-target, at room temperature), MCH concentrations from 0.00 to 1.00 mM were incubated for 30 min (**Figure 3B**). The best S/B ratio (77.68) was registered when an MCH concentration of 1.00 mM was applied. As for the MCH incubation time (**Figure 3C**), sensors incubated with MCH for 15, 30 and 60 min were tested. The highest S/B ratio (296.59), and consequently the highest intensities (I = 1.56 μA), were observed after 30 min of incubation, followed by the 15 min incubation period (S/B = 181.15 and I = 0.95 μA). On the other hand, the SPGEs incubated for a 60 min period presented the worst S/B (169.54) and I (I = 0.89 μA) values. This result is also in accordance with the literature; similar to the MCH concentration, lengthier MCH incubation times help with the DNA-capture probes orientation, as well as with the removal of weakly attached DNA sequences on the SPGE's surface. Nevertheless, incubation periods over 30 min normally result in a decrease of the analytical signal due to signal shifts and increased background noise [23,26].

3.3.2. Optimizations associated with the hybridization phase

As previously mentioned, a sandwich hybridization format was chosen for the design of this DNA-based biosensor. This strategy entails two independent hybridization events that increase the overall selectivity of the assay [22]. The first reaction results from the partial hybridization between the DNA-target sequences and the DNA-signaling probes, dubbed homogeneous hybridization. Whereas the second and complete hybridization, designated heterogeneous hybridization, occurs when the DNA-target/DNA-signaling hybrid is added to the DNA-capture probes fixated on the surface of the working electrode. Thus, to improve the analytical responses of the electrochemical genosensor during the hybridization phase, the heterogeneous incubation time, as well as the homogeneous incubation and temperature were tested (**Figure 4**).

For the heterogeneous hybridization reaction, the best S/B ratio value (288.72) and, coincidentally, the highest current intensity (I = 1.28 μA) were registered after an incubation period of 30 min (**Figure 4A**). Meanwhile, for the homogeneous hybridization optimization, a S/B ratio of 282.85 and a current intensity of 1.73 μA was obtained with a 30 min incubation (**Figure 4B**).

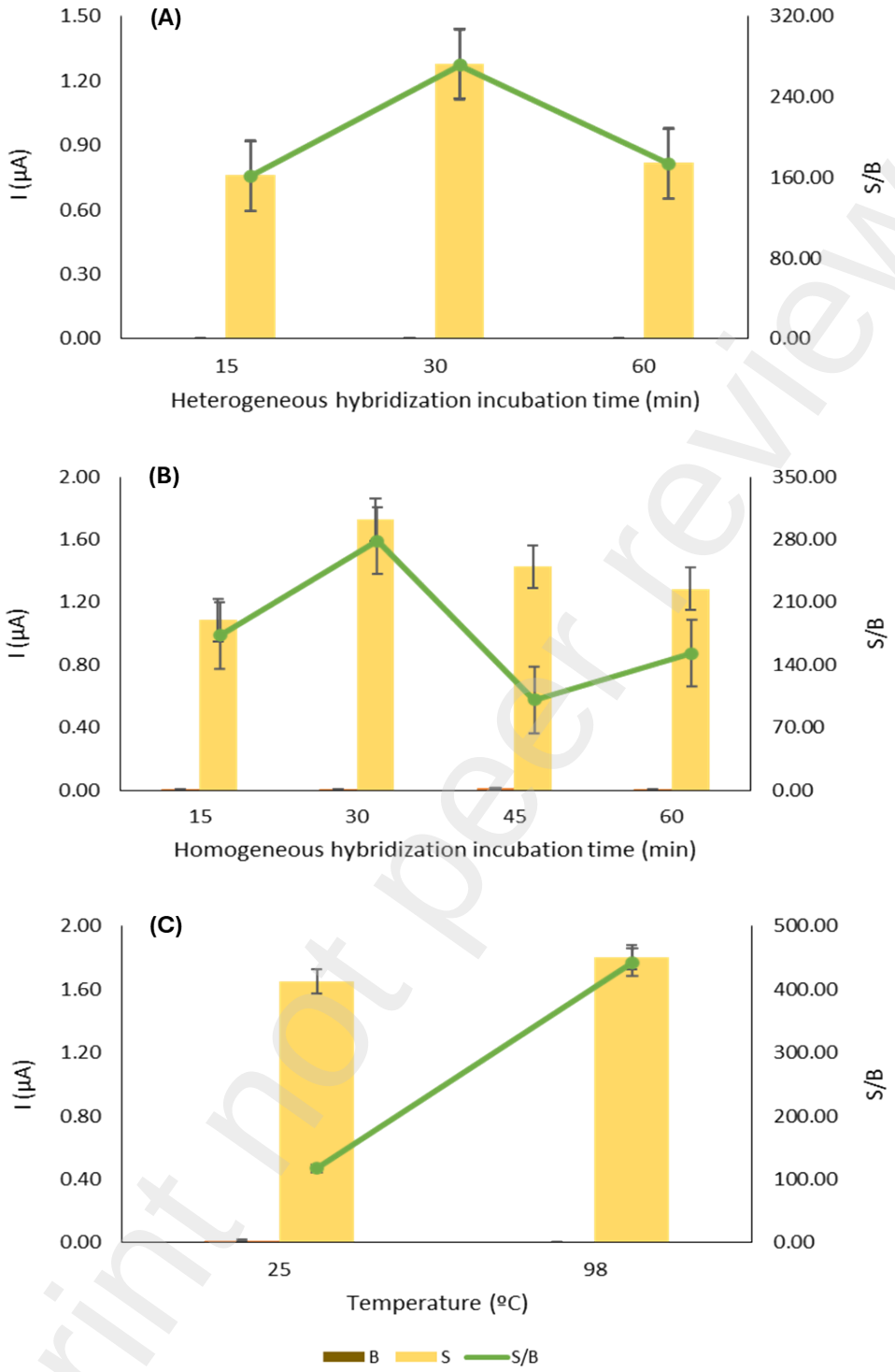

Figure 4. Influence of the (A) incubation time in the heterogeneous hybridization and (B) incubation time and (C) temperature in the homogeneous hybridization reaction. Blank values (B) represented in dark brown, signal (S) in light yellow and the corresponding S/B ratio in green. Error bars estimate the standard deviation of three replicates.

In molecular biology, before use, oligonucleotide sequences normally suffer a denaturation process by heating those sequences to 95 ± 1ºC for 5 min and then cooling them in an ice bath for another 5 min. This process facilitates the rupture of the DNA's double stranded structure [23]. Nonetheless, the *C. sativa* DNA sequences (**Table 1**) were designed to function at room temperature (approximately 25ºC ± 1ºC). So, to determine the influence of the homogeneous hybridization reaction temperature on the electrochemical signal two temperatures (25ºC and 98ºC) were assessed (**Figure 4C**).

As observed in **Figure 4C**, both temperatures attained similar current intensities (I = 1.65 at room temperature and I = 80 at 98ºC), nevertheless the assays that suffered the denaturation process present a higher S/B ratio (S/B = 447.33). Therefore, all further analysis will be performed after a denaturation process.

3.3.3. Optimization of the detection phase

The final three optimizations (signaling probes concentration and the Anti-FICT-POD concentration and incubation time), are those directly associated with the detection of the enzymatic amplification of the electrochemical signal (**Figure 5**). This amplification is the result of a redox reaction between the antibody's peroxidases (Anti-FICT-POD, which attached themselves to the fluorescein molecule of the DNA-signaling probe), and the TMB/H_2O_2 complex. Hence, the first optimization in this process is the concentration of the DNA-signaling probe (**Figure 5A**).

In this case, increasing concentrations from 12.50 to 50.00 μM of DNA-signaling were used to study the influence of the signaling probes concentration on the electrochemical responses. As visible in **Figure 5A**, the best S/B ratio (131.24) and Ic (1.77 μA) were registered when 25.00 μM of the DNA-signaling probe was added to the system, followed by the 12.50 μM concentration with a S/B ratio and Ic of 116.28 and 1.57 μA, respectively. Thus, the worst values were recorded when 50.00 μM of the DNA-signaling probes were used (S/B = 94.96 and Ic = 1.28 μA).

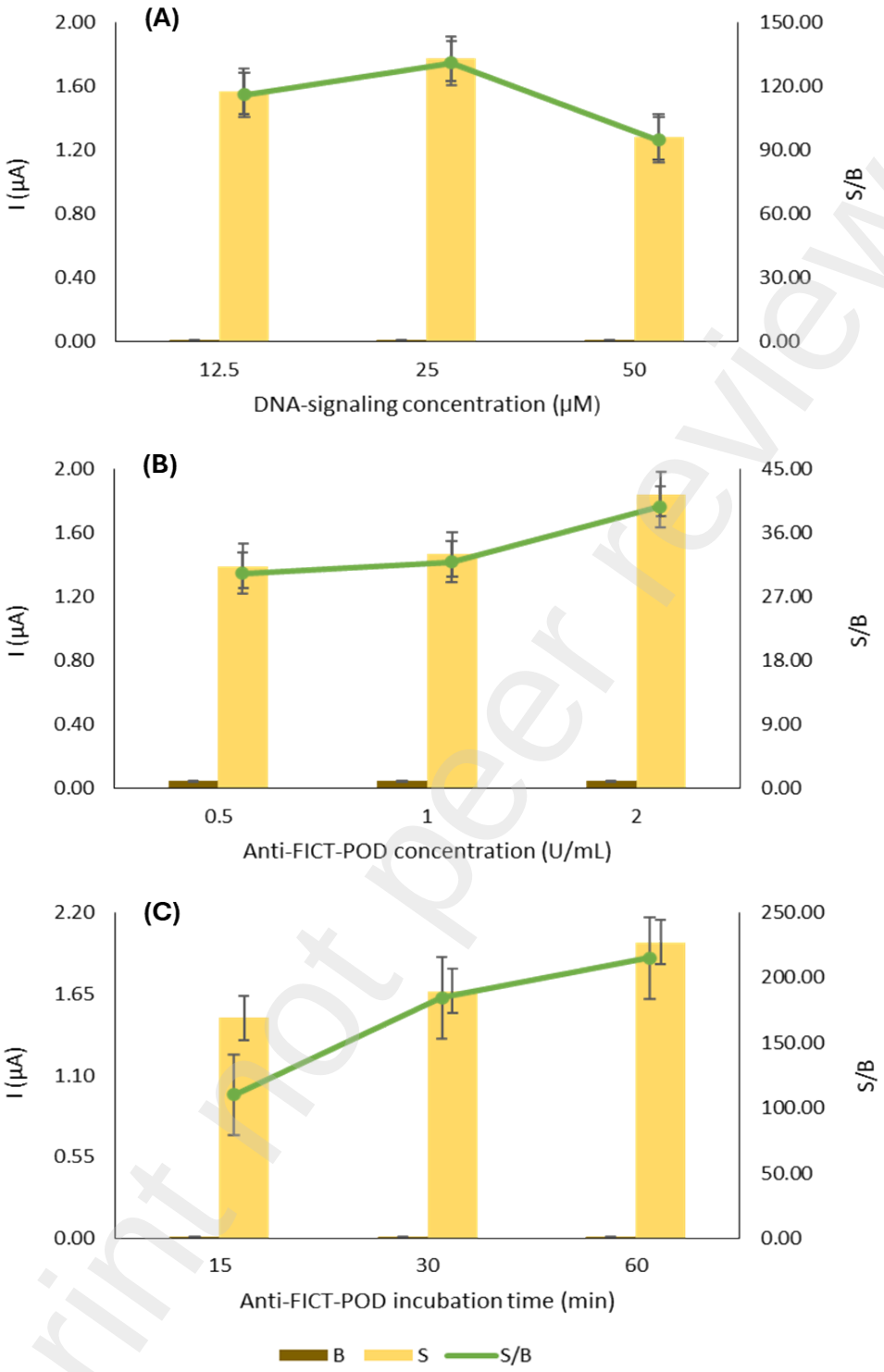

Figure 5. Chronoamperometric responses acquired when optimizing the concentration of the DNA-signaling probe (A), and the concentration (B) and incubation time of the Anti-FICT-POD (C). Blank values (B) represented in dark brown, signal (S) in light yellow and the corresponding S/B ratio in green. Error bars estimate the standard deviation of three replicates.

Finally, the Anti-FICT-POD concentration and incubation time were analyzed (**Figure 5B** and **5C**, respectively). This is an important optimization parameter since, theoretically, when the TMB/H_2O_2 complex is applied for the electrochemical detection of the hybridization reaction, the amount of POD enzymes should be directly proportional to the number of hybridized sequences on the electrode's surface [22]. Therefore, to determine the influence of the anti-FITC-POD

enzymes on the genosensor's performance, three different concentrations of the antibody, ranging from 0.5 to 2.0 U/mL, were incubated on the DNA-based biosensor, over a 15-, 30-, and 45-min incubation period.

As observed in **Figure 5B**, the increase in the Anti-FICT-POD enzyme concentration led to an increase of both the S/B ratios, as well as the Ic. So, the values for the S/B ratios and Ic were 30.25 and 1.39, 31.91 and 1.47, and 39.65 and 1.84 for the 0.50, 1.00 and 2.00 U/mL antibody concentrations. Similarly, for the incubation time of the Anti-FICT-POD (**Figure 5C**), increasing the incubation time of the antibody on the electrode's surface resulted in an increase of the chronoamperometric signal response. The best S/B (215.16) was registered after a 60 min incubation period.

Table 2. Selected values for the electrochemical genosensor construction.

Variables	Tested range	Selected value
DNA Capture probe concentration (µM)	0.25–10.00	1.00
MCH concentration (µM)	0.00–1.00	1.00
MCH incubation time (min)	15–60	30
Homogeneous hybridization incubation time (min)	15–60	30
Temperature (ºC)	25-98	25
DNA-signaling concentration probe (µM)	0.13–0.50	0.25
Heterogeneous hybridization incubation time (min)	15–60	30
Antibody concentration (U/mL)	0.50–2.00	2.00
Antibody incubation time (min)	15–60	60

3.4. Analytical characteristics

Under the optimal analytical conditions (**Table 2**), the performance of the developed genosensor was assessed by chronoamperometry using increasing concentrations (0.03 to 5.00 nM) of the chestnut-specific DNA-target probe (**Figure 6**). A linear relationship (R^2 = 0.992) between the blank-subtracted current intensity and the synthetic *C. sativa* DNA-target concentration was obtained in a 0.03 – 1.00 nM range, with a slope and intercept value of 1.532 ± 0.04 (µA/nM) and 0.037 ± 0.01 (µA), respectively.

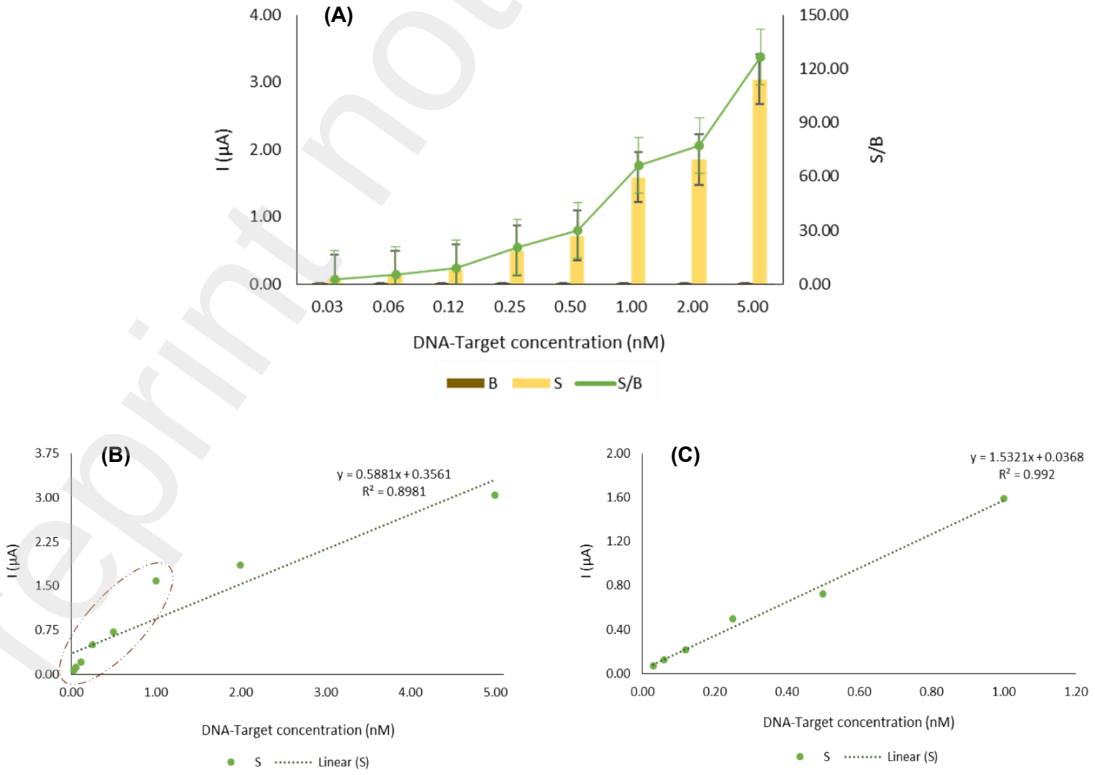

Figure 6. Chronoamperometric responses for (A) the blank subtracted synthetic DNA-target current intensities and calibration curve (B) ranging from 0.03 to 5.00 nM and (C) 0.03 to 1.00 nM. Current responses obtained from an average of three replicates.

A limit of detection (LOD) of 3.01 pM and a limit of quantitation (LOQ) of 10.04 pM were obtained (**Table 3**). The LOD and LOQ were calculated as three and ten times the estimated standard deviation from the chronoamperometric measurements registered in the absence of the DNA-target (i.e., blank assays) divided by the value of the linear calibration slope, respectably.

Additionally, a repeatability of 2.49%, a reproducibility of 2.90% and total precision of 4.08% were attained (**Table 3**). The repeatability, reproducibility and total precision of the electrochemical genosensor were determined using five electrodes' measurements immobilized with the blank assay over a five-day period.

Table 3. Analytical parameters of the developed genosensor.

Parameters	Results
Linearity (nM)	0.03 – 1.00
Slope	1.53
Interception	0.04
Correlation (R)	0.992
Slopes' standard deviation	0.04
Interceptions' standard deviation	0.01
LOD (pM)	3.01
LOQ (pM)	10.04
Repeatability^n (%)	2.49
Reproducibility^n (%)	2.90
Total precision (%)	4.08

n = 5

3.5. Selectivity and sensitivity

After selecting the optimized analytical parameters (**Table 2**), the genomic DNA of the *C. sativa* plant was evaluated. The genomic DNA was extracted from *C. sativa* provided by the Natural Park of Montesinho (Bragança, Portugal) with the synthetic capture and signaling probes. Before use, the amplified fragments had suffered a denaturation process carried out by heating these oligonucleotide sequences to 95 ± 1ºC for 5 min and then cooling them down in an ice bath for another 5 min. This is a compulsory step due to the DNA's natural double stranded nature [23]. Then the denatured amplified DNA were mixed with the signaling probes to trigger the homogeneous hybridization reaction.

The genomic DNA extracted from C. sativa was diluted from the original to concentrations ranging from 0.13 to 1.00 nM. To test the sensor sensitivity, the diluted samples were applied and compared to the previously obtained calibration curve (**Figure 7**). A linear relationship (R^2 = 0.9902) between the current intensity and the amplified *C. sativa* plant DNA concentration was obtained in a 0.03 – 1.00 nM range, with a slope and intercept value of 1.1446 ± 0.03 (μA/nM) and 0.0852 ± 0.01 (μA), respectively.

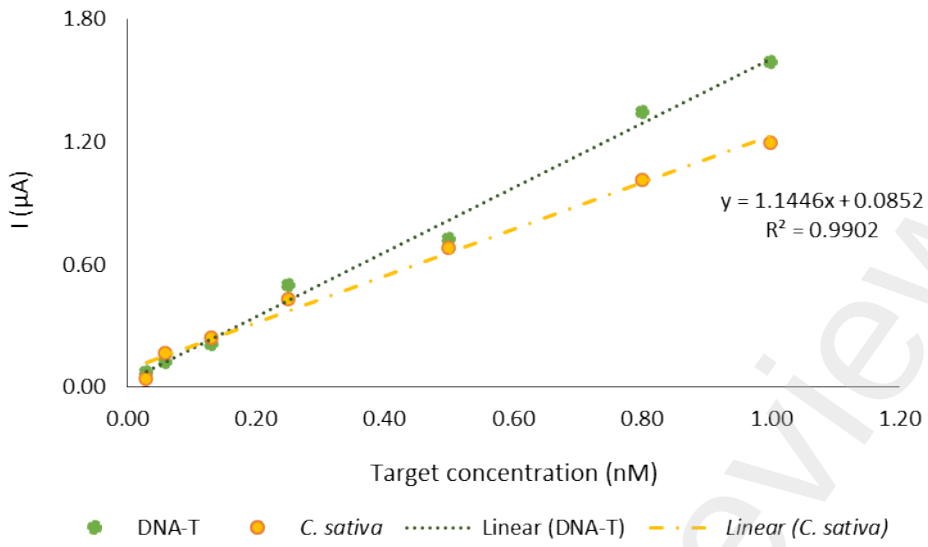

Figure 7. Comparison between the current intensities obtained from the synthetic DNA-Target probes and the genomic DNA extracted and amplified from *Castanea sativa* plant samples. Green and yellow dots correspond to the synthetic DNA-target probes and the amplified genomic *C. sativa* DNA, respectively. Error bars estimate the standard deviation of three replicates.

As observed in **Figure 7**, increasing the concentration of the amplified DNA results in lower current intensities than the synthetic DNA-target sequences. The greater differences between the two current intensities are visible from the 0.80 nM and 1.00 nM genomic DNA concentrations, which present, respectively, a 24.75% and 24.81% deviation from DNA-target probes. Only the lower DNA concentrations (0.03 – 0.50 nM) report current intensities values closer to those from the synthetic probes.

3.6. Authentication of commercial honey samples

Following the previously mentioned protocol, the DNA extracted from twelve commercial honey samples were amplified and quantified. To determine the presence of *C. sativa* in the twelve samples, their amplified DNA was reduced to 1.00 nM and applied to the developed sensor. The result from the enzymatic amplification of the electrochemical signal is visible in **Figure 8**.

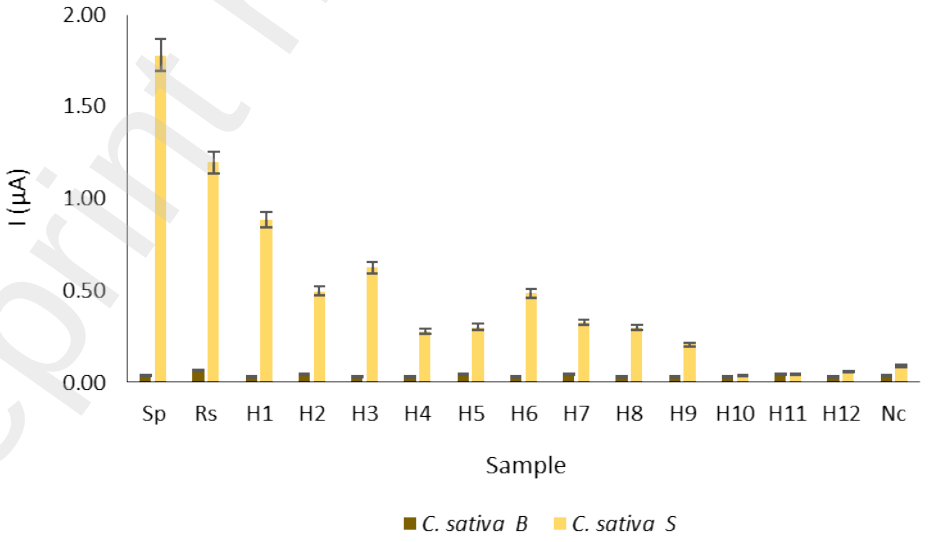

Figure 8. Comparison between the electrochemical signals registered from the synthetic DNA-target (Sp) and *Castanea sativa* plant DNA (Rs) with the DNA extracted from twelve commercial honey samples (H1- H12) and the non-

complementary DNA (Nc). Current values of the blank assays (B) in beige and electrochemical signals (S) in yellow. All measurements were performed with a DNA concentration of 1.00 nM. Error bars estimate the standard deviation of three replicates.

The highest current intensity was registered by the synthetic DNA-target probe (I = 1.78 µA), followed by the genomic DNA extracted from the *C. sativa* plant (I = 1.20 µA). As for the commercial honey samples, the decreasing order of intensities was 0.88 µA, 0.63 µA, 0.50 µA, 0.48 µA, 0.33 µA, 0.30 µA, 0.30 µA, 0.28 µA, 0.21 µA, 0.06 µA, 0.05 µA and 0.04 µA for samples H1, H3, H2, H6, H7, H5, H8, H4, H9, H12, H11 and H10, respectively. Incidentally, the non-complementary (Nc) sequence registered a current intensity of 0.09 µA; an intensity slightly higher than samples H10, H11 and H12. This intensity difference can be attributed to noise in the electrochemical current or to some non-specific activity due to a trace contamination in the Nc sample.

Unfortunately, no monofloral-labeled chestnut honeys were obtained for this study. Samples H2 to H4 are commercialized as chestnut and heather flower honeys, while the other samples are either multifloral honeys (H6, H8, H9, H11, H12) or a specific flower honey (H1, H5, H7 and H10). So, even as an over-represented species, it is evident that their intensities will not reach the 80% range. Moreover, the difference in intensities between the three chestnut and heather honeys (H2 – H4) can be attributed to the prevalence of the chestnut trees in the area and harvest season of the honeys (**Table 3**). According to the literature, the botanical composition of honey also varies depending on the season/month that it is harvested [15]. So, additional studies are recommended to validate these results.

Table 3. Portuguese honey bloom calendar [adapted from: 15].

Bloom	Jan	Fev	Mar	Apr	May	Jun	Jul	Agu	Set	Oct	Nov	Dez
Arbutus unedo												
Echium plantagineum												
Erica arborea												
Erica umbellate												
Castanea sativa												
Eucaliptus globulus												
Helianthus annuus												
Lavandula stoechas												
Citrus sinensis												
Quercus pyrenaica												

3.7. Genosensor validation

Conventional PCR coupled with a gel electrophorese and RT-qPCR were then employed to validate the results obtained from the developed electrochemical genosensor. The genomic DNA from the *C. sativa* plant samples as well as the pollen DNA from the commercial honey samples were extracted in accordance with the protocol from Brion and the DNA yield and purity determined by a microplate spectrophotometer. For both methods, different melting temperatures (58°C and 62°C) were analyzed against the genomic DNA extracted from the plant samples and five commercial honey samples to obtain the best annealing temperature for *C. sativa*. For the conventional PCR analysis, the amplification results of all twelve samples were visualized with gel electrophorese. As for RT-qPCR only samples five were amplified. This selection was based on the knowledge of the geographical origin of the samples and resulting current intensity values.

3.7.1. Conventional PCR

To determine the best annealing temperature for the *C. sativa* amplification, several PCR runs were performed. Then a 2% agarose gel electrophorese was employed to verify the length of the

amplified DNA fragments. The image of the electrophorese run was obtained by the Gel Doc XR Imaging System (**Figure 9**).

Figure 9. Image obtained from the gel electrophorese run with the *Castanea sativa* plant and honey samples amplified by conventional PCR.

Conventional PCR is the gold standard for this type of molecular biology study. Nevertheless, as observed in **Figure 9**, little to no amplification was visible. This suggests that the conventional PCR is not as sensitive as the developed electrochemical genosensor, since this technique cannot detect the presence of DNA in lower concentrations. For that reason, conventional PCR is not an adequate analytical tool to authenticate the botanical origin of honeys.

3.7.2. Real-time quantitative PCR

To validate the functionality of three primer pairs targeting *C. sativa*, RT-qPCR was performed using SYBR Green detection with annealing temperatures of 62°C for the *Castanea* primers, as previously mentioned. Amplification was successfully obtained for all tested samples (plant and honey samples), and Ct values are summarized in **Table 4**.

Table 4: Ct values obtained for the tested samples using three primer pairs targeting *Castanea sativa*.

Sample	*Castanea* (Ct)
Rs	28.43
H1	30.94
H3	27.26
H4	28.30
H5	26.79
H7	28.17
H11	27.95
Nc	34.41

As observed in **Table 4**, the DNA amplification was successfully obtained for all the tested samples, including the non-complementary sample (Nc). For all reactions, the melting curve analysis revealed single, well-defined peaks, confirming the specificity of the amplified products. So, compared to the conventional PCR, RT-qPCR is more sensitive as it was able to visibly prove the extraction of the genomic DNA of each honey sample. Moreover, the amplification efficiency, calculated from the standard curve, fell within the acceptable range for RT-qPCR assays (90–110%). Together, these results confirm that the designed primer pairs are functional and suitable for the detection of their respective targets.

The highest Ct value (34.41) was obtained for the amplification of the extracted genomic DNA of the *E. arborea* plant (Nc) sample. According to the literature, the lower the Ct value the higher the initial DNA concentration of the desired target region [27]. Moreover, Ct values between 25 – 28 are usually considered the ideal for the amplification of genetic material; any sample over 28 cycles can lead to the detection of non-specific sequences due to the inactivation of the Taq polymerase [27,28]. In this case, the sample with the lowest Ct value (26.79) was sample H5 – commercially labeled as lavender honey. As an under-represented species, it is possible that the other main plant species present in the lavender honey is *C. sativa*.

Detecting the botanical DNA from any plant species in honey can be tricky because most of the DNA found in its mix is normally damaged and in small quantities [18]. Therefore, the application of molecular biological techniques, such as conventional PCR, can mitigate this problem by increasing the concentration of DNA from each honey. Nevertheless, as shown in **Figure 9**, the amplification of the genomic DNA from the plant and honey samples by conventional PRC was not able to confirm the presence of *C. sativa*. These findings suggest that conventional PRC is not as sensitive to low concentrations as the developed genosensor.

4. Conclusions

An electrochemical genosensor capable of detecting the genomic DNA of *C. sativa* was developed. The developed sensor was successfully applied for the detection and quantification of chestnut DNA in plant and honey samples, demonstrating its ability to discriminate between the real *C. sativa* DNA samples and the non-complementary DNA.

The sensor's design contributed to enhance its sensitivity, due to the self-assembled monolayer (composed of the thiolated-DNA-capture probe and MCH spacer), and selectivity from the employed sandwich hybridization strategy, obtaining a repeatability, reproducibility and total precision of 2.49%, 2.90% and 4.08%, respectively. When compared to the molecular methods (conventional PCR and RT-qPCR) the total analysis time of the developed genosensor, after the overnight immobilization, is comparable to that of the molecular techniques. Nonetheless, the genosensor offers a greater analytical performance as it can detect and quantify DNA concentrations as low as 0.03 nM. This result makes the genosensor an especially viable method for honey DNA since its extraction normally generates a low DNA concentration, often hindering the visualization of any amplified products by gel electrophorese.

Moreover, in the case of the RT-qPCR analysis, all samples were successfully amplified, with Ct values between 26.79 and 34.41 for the *C. sativa*-specific primers. These results corroborate the effectiveness of the developed genosensor, which, unlike the conventional PCR, was capable of detecting the presence of the amplified chestnut DNA. In terms of price, a DNA-based biosensor is more affordable than the RT-qPCR method. Hence, electrochemical genosensors are a promising analytical tool to address honey fraud, by facilitating honey authenticity and enhancing food safety.

CRediT authorship contribution statement

Stephanie L. Morais: Data curation, Formal analysis, Investigation, Methodology, Validation, Visualization, Writing – original draft. **Eduarda Pereira**: Data curation, Formal analysis, Investigation, Methodology, Validation, Visualization. **Mariana Fereira**: Data curation, Formal analysis, Investigation, Validation, Visualization, Writing – original draft. **Marlene Santos**: Conceptualization, Investigation, Resources, Supervision. **Sónia Soares**: Methodology, Resources, Writing – review & editing. **Ana L. Teixeira**: Formal analysis, Investigation, Methodology, Resources, Supervision, Validation, Visualization, Writing – review & editing. **Valentina F. Domingues**: Conceptualization, Resources, Supervision, Writing – review & editing. **Cristina Delerue-Matos**: Conceptualization, Funding acquisition, Project administration, Supervision, Visualization, Writing – review & editing. **M. Fátima Barroso**: Conceptualization, Supervision, Funding acquisition, Project administration, Resources, Supervision, Visualization, Writing – review & editing. All authors have read and agreed to the published version of the manuscript.

Declaration of competing interest

The authors declare that they have no known competing financial interests or personal relationships that could have appeared to influence the work reported in this paper.

Acknowledgements

This work received financial support from the PT national funds (FCT/MECI) through the project UID/50006/2025 DOI 10.54499/UID/50006/2025 -Laboratório Associado para a Química Verde - Tecnologias e Processos Limpos and from the project "Challenging the Analytical Diagnosis of Neurodevelopmental Disorders: Pioneering Neurochemical Devices", funded by FEDER funds and PT funds by FCT/MECI, operation no. 15875, with reference COMPETE2030-FEDER-00699000, and by the project Chestfilm, supported by "La Caixa" Foundation and FCT through the 4th edition of the Promove program "O Futuro do Interior.

M.Fátima Barroso thanks the TENURE – FCT Tenure Program – 1st Edition (Reference 2023.15797.TENURE.001) with financial support from FCT/MCTES through national funds. S. Soares thanks FCT (Fundação para a Ciência e a Tecnologia) for funding through the Scientific Employment Stimulus—Individual Call CEECIND/00588/2022 DOI: 10.54499/2022.00588.CEECIND/CP1724/CT0009). Stephanie Morais (2023.028929.BD) and Eduarda Pereira (2024.01697.BDANA) are grateful to FCT and the European Union (EU) for their grants financed by POPH-QREN-Tipologia 4.1-Formação Avançada, funded by Fundo Social Europeu (FSE) and Ministério da Ciência, Tecnologia e Ensino Superior (MCTES).

Data availability

Data will be made available on request.

References

[1] R.K. Bannor, K.K. Arthur, D. Oppong, H. Oppong-Kyeremeh, A comprehensive systematic review and bibliometric analysis of food fraud from a global perspective. *J. Agric. Food Res.* 14 (2023) 100686. https://doi.org/10.1016/j.jafr.2023.100686

[2] G. Zhang, W. Abdulla, On honey authentication and adulterant detection techniques. *Food Cont*. 138 (2022) 108992. https://doi.org/10.1016/j.foodcont.2022.108992

[3] European Union. Regulation (EU) 2017/625 of the European Parliament and of the Council of 15 March 2017 on official controls and other official activities performed to ensure the application of food and feed law, rules on animal health and welfare, plant health and plant protection products. Official Journal of the European Communities - Legislation, 95:7.4 (2017) 1 – 142. https://eur-lex.europa.eu/eli/reg/2017/625/oj

[4] European Commission. The EU agri-food fraud network and the administrative assistance and cooperation system: 2020 annual Report. (2021). https://ec.europa.eu/food/document/download/5135ace4-2a9d-4bf7-afad-574621b43b1c_en

[5] R.A.N. Insha, N. Islam, M.N. Hasan, M. Rahman, Comprehensive honey authentication in Bangladesh: Profiling physicochemical and bioactive compounds to distinguish floral sources and detect adulteration. *Heliyon*. 10:21 (2024) e40203. https://doi.org/10.1016/j.heliyon.2024.e40203

[6] M. Milli, N.S. Milli, Í.H. Parlak, Rapid detection of honey adulteration using machine learning on gas sensor data, *NPJ, Sci. Food*. 9 (2025) 74. https://doi.org/10.1038/s41538-025-00440-9

[7] S. Soares, J.S. Amaral, M.B.P.P. Oliveira, I. Mafra, A Comprehensive Review on the Main Honey Authentication Issues: Production and Origin. *Compr. Rev. Food Sci. Food Saf*. 16:5 (2017) 1072 – 1100. https://doi.org/10.1111/1541-4337.12278

[8] M. Silva, M. Maia, M. Carvalho, A.N. Barros, Portuguese Monofloral Honeys: Molecular Insights and Biochemical Characterization. *Molecules*, 30:8 (2025) 1808. https://doi.org/10.3390/molecules30081808

[9] M.-A. Rodopoulou, C. Tananaki, D. Kanelis, V. Liolios, M. Dimou, A. Thrasyvoulou, A chemometric approach for the differentiation of 15 monofloral honeys based on physicochemical parameters. *J. Sci. Food Agric.* 102 (2022)139 – 146. https://doi.org/10.1002/jsfa.11340

[10] H.F. Abou-Shaara, R. Sciberras, An approach to protected designation of origin (PDO) for bee honey utilizing the normalized difference vegetation index (NDVI). *Remote Sens. Lett*. 15:10 (2024) 1057 – 1062. https://doi.org/10.1080/2150704X.2024.2398816

[11] A.-I. Glogoveţan, P. Šedík, C.B. Pocol, The Importance of Certification with PDO and PGI Quality Schemes: A Critical Analysis of the Romanian Beekeeping Sector. *Bull. Univ. Agric. Sci. Vet. Med. Cluj-Napoca, Food Sci. Technol*. 78 (2021) 35 – 43. https://doi.org/10.15835/buasvmcn-fst:2021.0024

[12] European Commission. Geographical indications food and drink: State of the Union (2025). Geographical indications and quality schemes explained - European Commission

[13] E. Bruneau, C. Adolphe, N.S. Delso, S. Spiewok, M. Rubinigg, European Honey Market, *EU Pollinator Hub.* (2024) 1 – 25. https://app.pollinatorhub.eu/articles/2

[14] A. Puścion-Jakubik, M.H. Borawska, K. Socha, Modern Methods for Assessing the Quality of Bee Honey and Botanical Origin Identification. *Foods*. 9:8 (2020) 1028. https://doi.org/10.3390/foods9081028

[15] FNAP – Federação Nacional dos Apicultores de Portugal, Programa Apícola Nacional, 2017-2019. Boletim estatístico, 2016.

[16] J. Ye, G. Coulouris, I. Zaretskaya, I. Cutcutache, S. Rozen, T.L. Madden, Primer-BLAST: A tool to design target-specific primers for polymerase chain reaction. *BMC Bioinform*. 13 (2012) 134. https://doi.org/10.1186/1471-2105-13-134

[17] J.J. Doyle, J.L. Doyle, A Rapid DNA Isolation Procedure for Small Quantities of Fresh Leaf Tissue. *Phytochem. Bull*. 19:1 (1987) 11 – 15.

[18] S. Soares, J. Amaral, M. Oliveira, I. Mafra, Improving DNA isolation from honey for the botanical origin identification. *Food Control*. 48 (2015) 130 – 136. https://doi.org/10.1016/j.foodcont.2014.02.035

[19] C.M.A. Brett, Electrochemical Impedance Spectroscopy in the Characterisation and Application of Modified Electrodes for Electrochemical Sensors and Biosensors. *Molecules*. 27 (2022) 1497. https://doi.org/10.3390/molecules27051497

[20] H. Kazemzadeh-Beneh, M.R. Safarnejad, P. Norouzi, D. Samsampour, S.M. Alavi, D. Shaterreza, Development of label-free electrochemical OMP-DNA probe biosensor as a highly sensitive system to detect of citrus huanglongbing. *Sci. Rep.* 14 (2024) 12183. https://doi.org/10.1038/s41598-024-63112-w

[21] S. Cho, Y. Oh, S.M. Ahn, Influence of DNA concentration on the interfacial electrode impedance. *J. Nanosci. Nanotechnol*. 13:11 (2013) 7291 – 7294. https://doi.org/10.1166/jnn.2013.8085

[22] M.F. Barroso, M. Freitas, M.B.P.P. Oliveira, N. de-los-Santos-Alvarez, M.J. Lobo-Castañon, C. Delerue-Matos, 3D-nanostructured Au electrodes for the event-specific detection of Mon810 transgenic maize, *Talanta*. 134 (2015) 158 – 164. https://doi.org/10.1016/j.talanta.2014.10.017

[23] S. Campuzano, F. Kuralay, M.J. Lobo-Castañon, M. Bartosík, M.K. Vyavahare, E. Palecek, D.A. Haake, F. Wang, Ternary monolayers as DNA recognition interfaces for direct and sensitive electrochemical detection in untreated clinical samples. *Biosens. Bioelectron*. 26 (2011) 3577 – 3583. https://doi.org/10.1016/j.bios.2011.02.004

[24] L. Zhang, Z. Li, X. Zhou, G. Yang, J. Yang, H. Wang, M. Wang, C. Liang, Y. Wen, Y. Lu, Hybridization performance of DNA/mercaptohexanol mixed monolayers on electrodeposited nanoAu and rough Au surfaces, *J. Electroanal. Chem*. 757 (2015) 203 – 209. https://doi.org/10.1016/j.jelechem.2015.09.032

[25] X. Xu, A. Makaraviciute, S. Kumar, C. Wen, M. Sjödin, E. Absurakhmanov, U.H. Danielson, L. Nyholm, Z. Zhang, Structural Changes of Mercaptohexanol Self-Assembled Monolayers on Gold and Their Influence on Impedimetric Aptamer Sensors. *Anal. Chem.* 91 (2019) 14697 – 14704. https://doi.org/10.1021/acs.analchem.9b03946

[26] H. Sohrabi, M.R. Majidi, K. Asadpour-Zeynali, A. Khataee, A. Mokhtarzadeh, Self-assembled monolayer-assisted label-free electrochemical genosensor for specific point-of-care determination of Haemophilus influenzae. *Microchim. Acta*. 190 (2023) 112. https://doi.org/10.1007/s00604-023-05687-1

[27] J. Shanmughanandhan, D. Shanmughanandhan, S. Ragupathy, T.A: Henry, S.G. Newmaster, Quantification of *Actaea racemosa* L. (black cohosh) from some of its potential adulterants using qPCR and dPCR methods. *Sci. Rep*. 11 (2021) 4331. https://doi.org/10.1038/s41598-020-80465-0

[28] W.F., Sule, D.O. Oluwayelu, Real-time RT-PCR for COVID-19 diagnosis: challenges and prospects. *Pan. Afr. Med. J.* 35 (2020) 121. https://doi.org/10.11604/pamj.supp.2020.35.24258

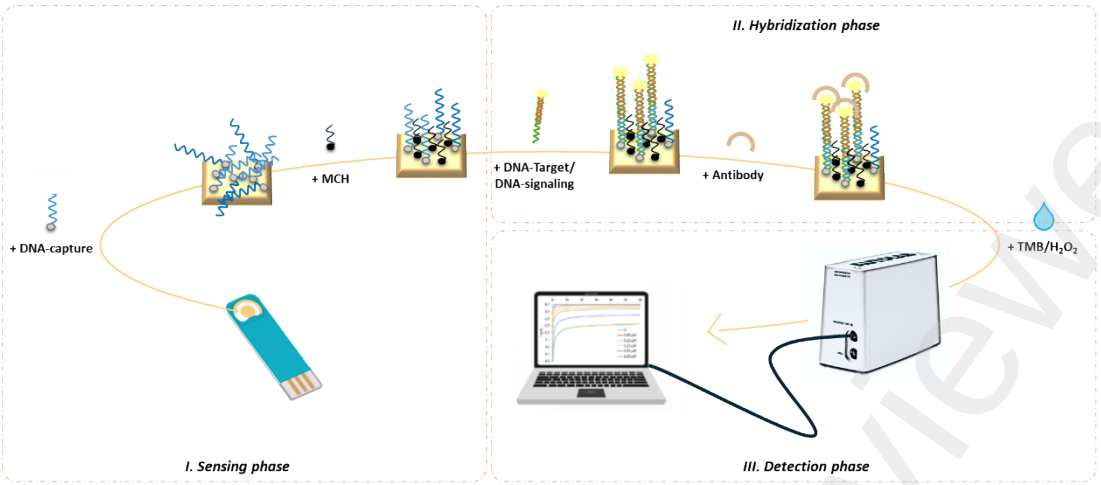

Figure 1. General design of the electrochemical genosensor.

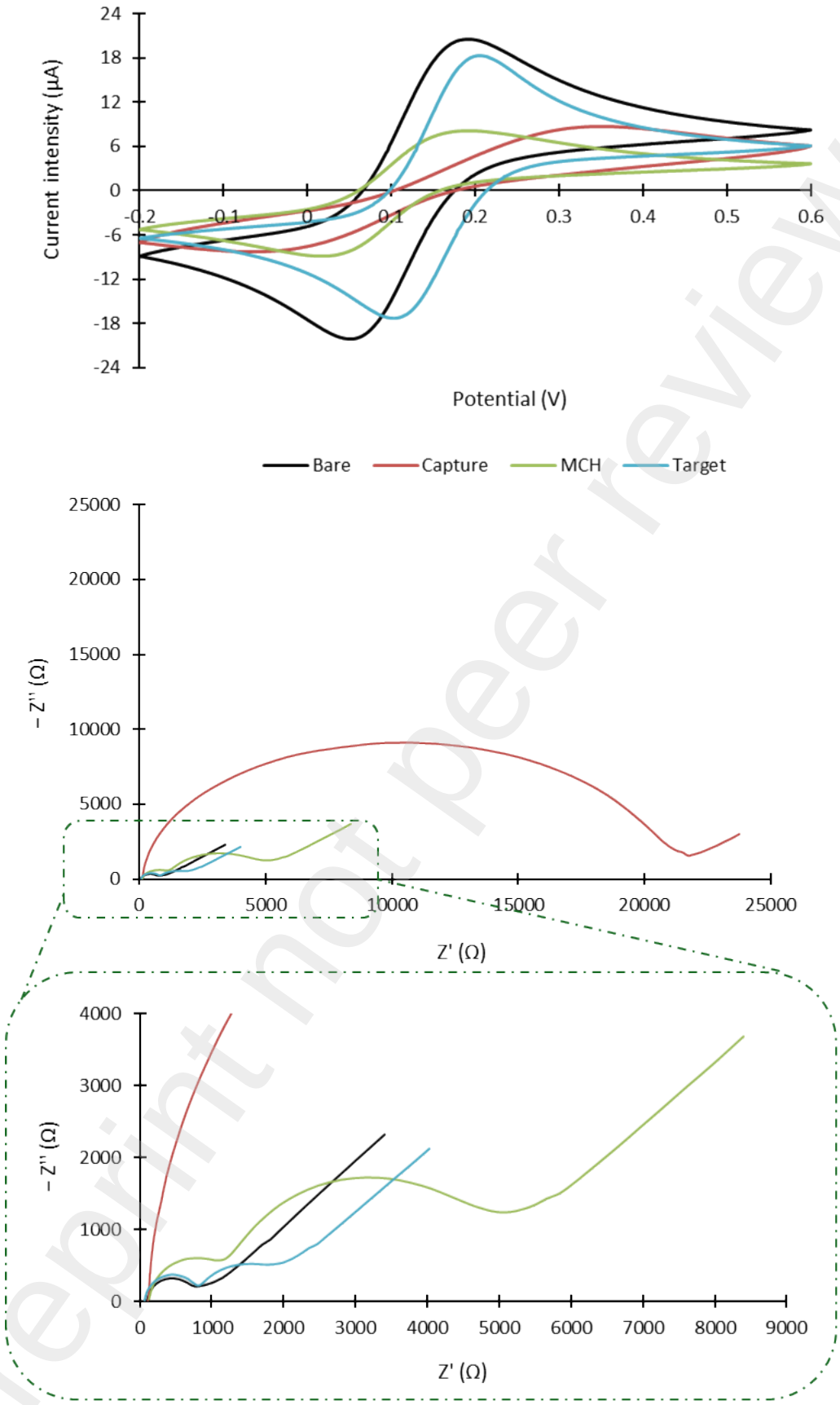

Figure 2. Characterization of the bare gold (Au) (black), DNA-capture modified (Au/DNA-capture, red), mercaptohexanol modified (Au/DNA-capture/MCH, light green) and doble stranded (dsDNA) hybrid (Au/DNA-capture/MCH/DNA-target/DNA-signaling, light blue) electrode surface by cyclic voltammograms (A) and Nyquist plots resulting from electrochemical impedance spectroscopy (B). All measurements were recorded at 2.50 mM $[Fe(CN)_6]^{-3/-4}$ prepared in KCl.

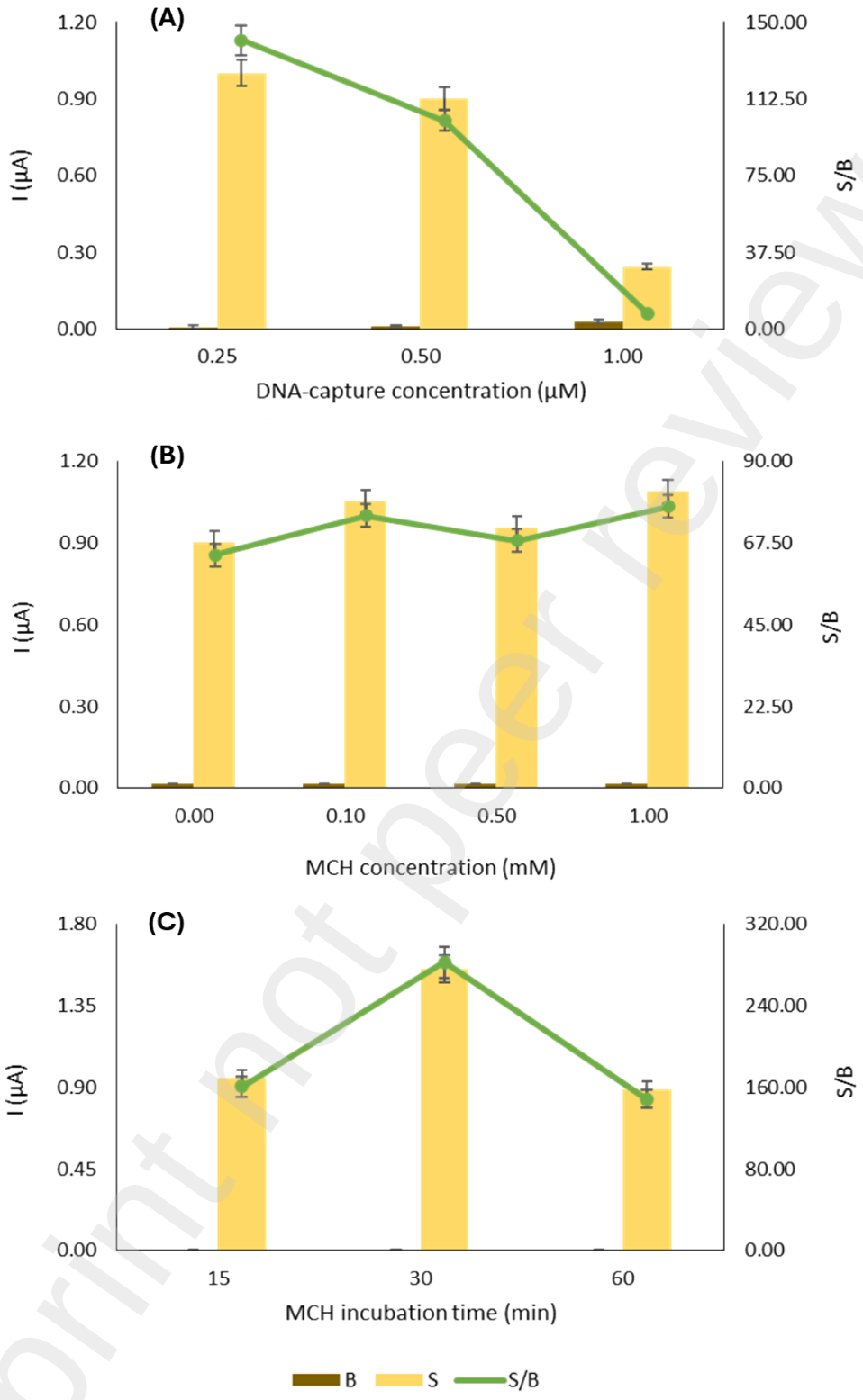

Figure 3. Chronoamperometric responses acquired when optimizing the concentration of the DNA-capture probe (A), and the concentration (B) and incubation time of MCH (C). Blank values (B) represented in dark brown, signal (S) in light yellow and the corresponding S/B ratio in green. Error bars estimate the standard deviation of three replicates.

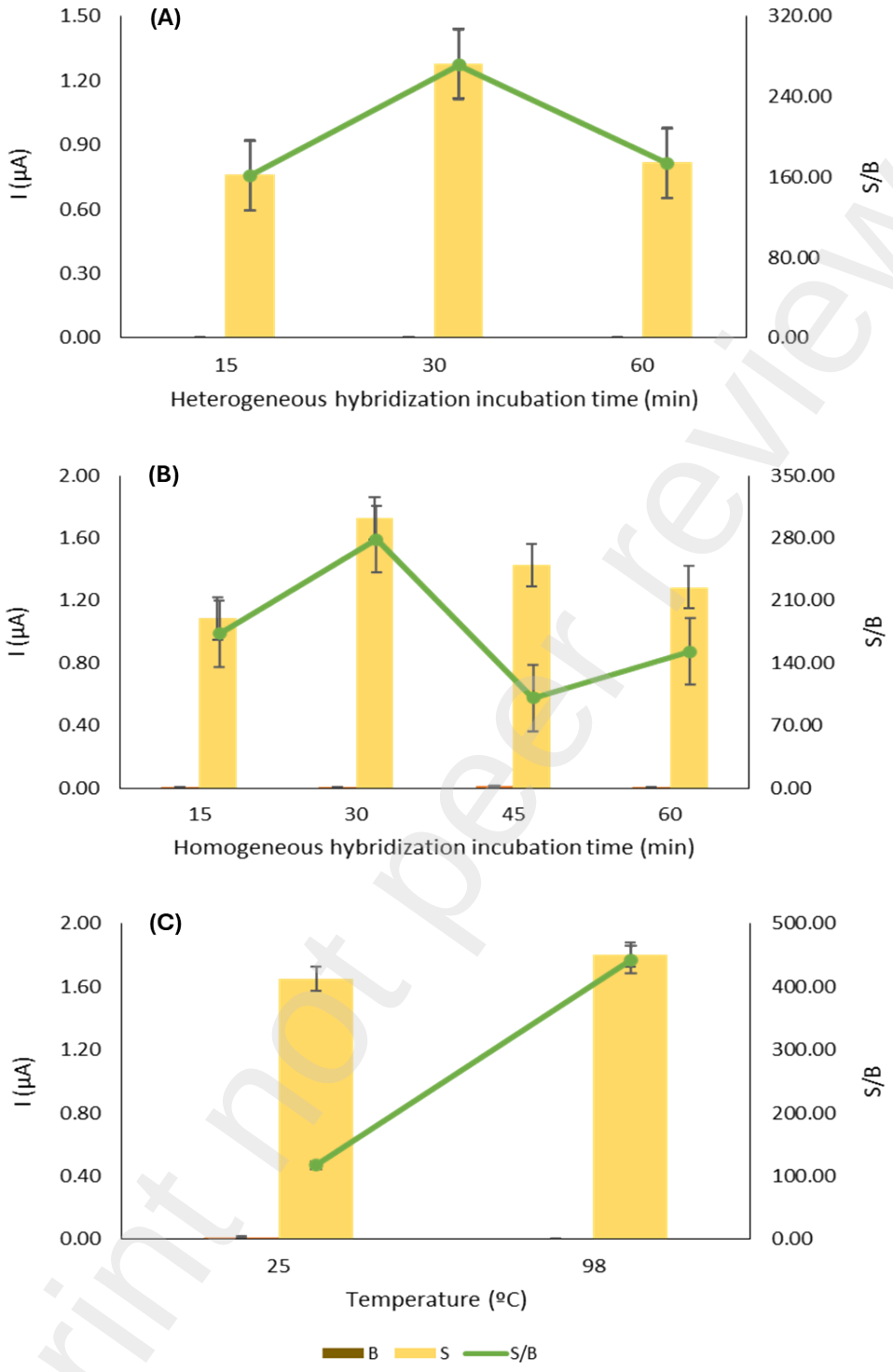

Figure 4. Influence of the (A) incubation time in the heterogeneous hybridization and (B) incubation time and (C) temperature in the homogeneous hybridization reaction. Blank values (B) represented in dark brown, signal (S) in light yellow and the corresponding S/B ratio in green. Error bars estimate the standard deviation of three replicates.

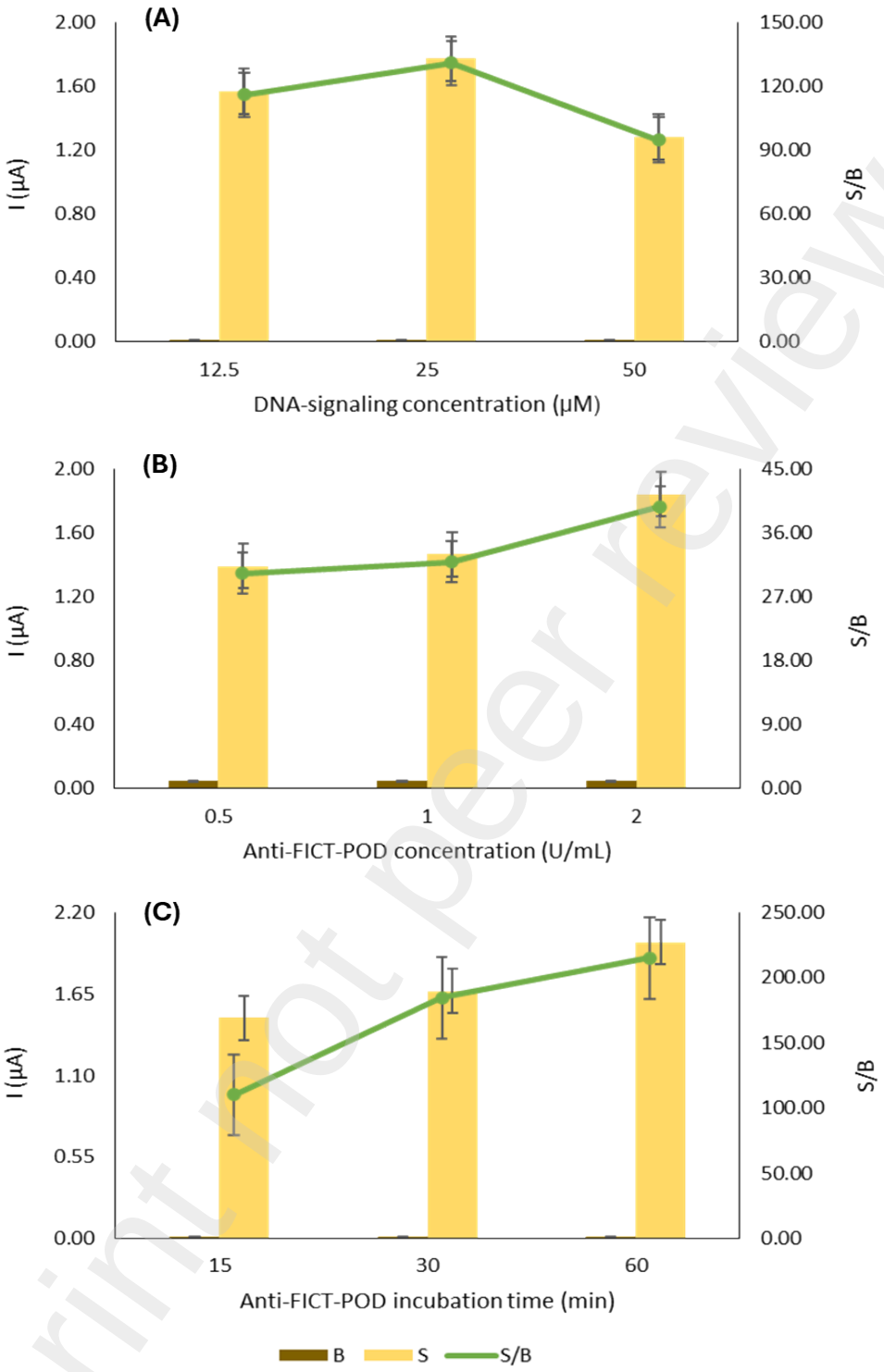

Figure 5. Chronoamperometric responses acquired when optimizing the concentration of the DNA-signaling probe (A), and the concentration (B) and incubation time of the Anti-FICT-POD (C). Blank values (B) represented in dark brown, signal (S) in light yellow and the corresponding S/B ratio in green. Error bars estimate the standard deviation of three replicates.

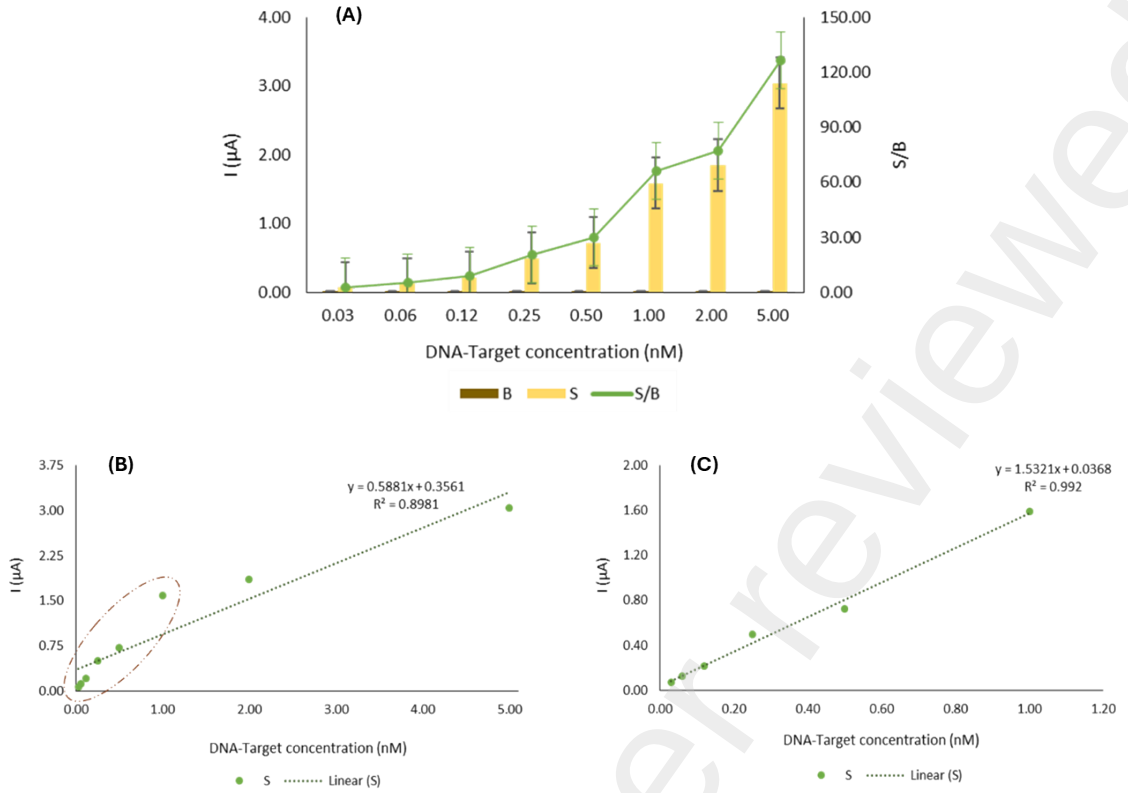

Figure 6. Chronoamperometric responses for (A) the blank subtracted synthetic DNA-target current intensities and calibration curve (B) ranging from 0.03 to 5.00 nM and (C) 0.03 to 1.00 nM. Current responses obtained from an average of three replicates.

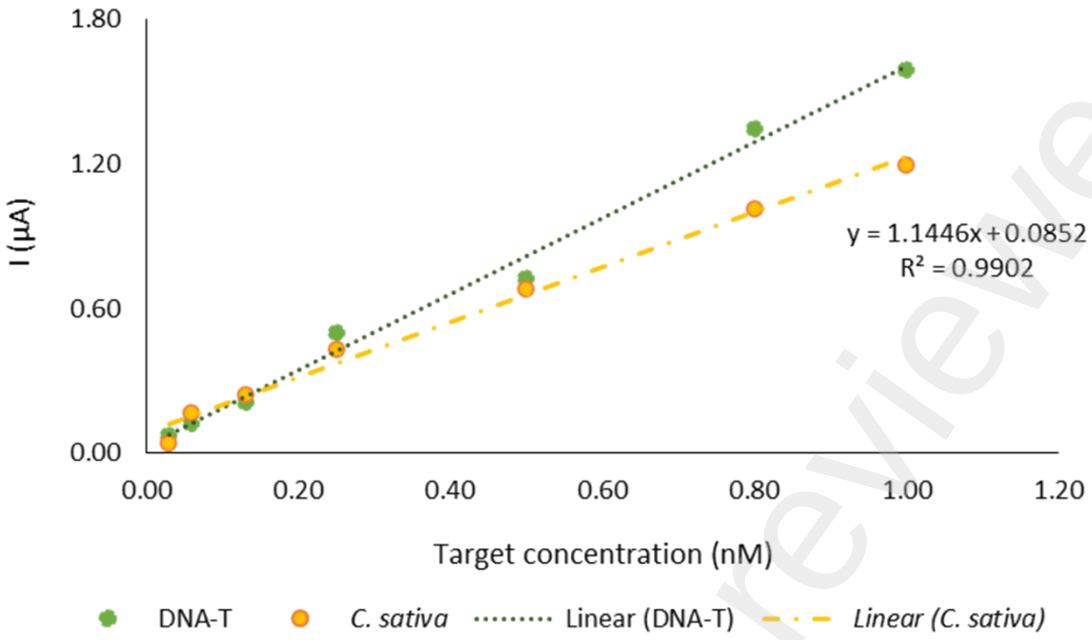

Figure 7. Comparison between the current intensities obtained from the synthetic DNA-Target probes and the genomic DNA extracted and amplified from *Castanea sativa* plant samples. Green and yellow dots correspond to the synthetic DNA-target probes and the amplified genomic *C. sativa* DNA, respectively. Error bars estimate the standard deviation of three replicates.

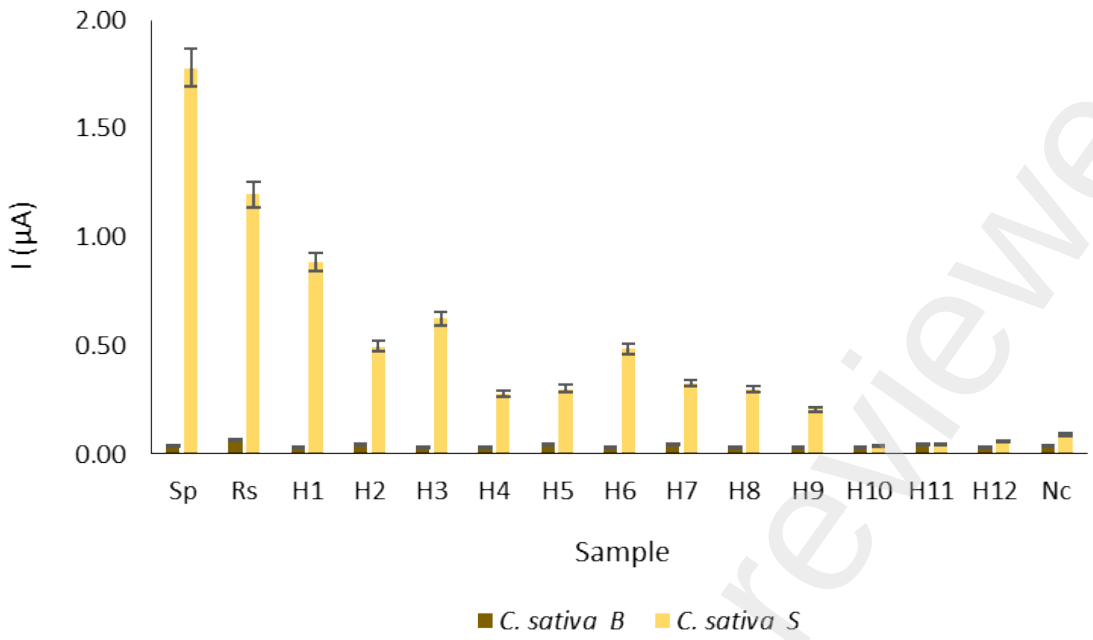

Figure 8. Comparison between the electrochemical signals registered from the synthetic DNA-target (Sp) and *Castanea sativa* plant DNA (Rs) with the DNA extracted from twelve commercial honey samples (H1- H12) and the non-complementary DNA (Nc). Current values of the blank assays (B) in beige and electrochemical signals (S) in yellow. All measurements were performed with a DNA concentration of 1.00 nM. Error bars estimate the standard deviation of three replicates.

Figure 9. Image obtained from the gel electrophorese run with the *Castanea sativa* plant and honey samples amplified by conventional PCR.

Table 1. Oligonucleotide sequences designed for *Castanea sativa*.

Oligonucleotide	Sequence 5' → 3'	Base pairs (bp)
DNA- capture	**SH**-ATC AGA GGA TGA GTG GGA CCA C	22
DNA-signalling	CTA TAA AAT TTC ATG ACT CTA TGA ATT GTG TGT GTG TGT GTG TGT GTG GGG AGA TTT CCA TTG ATA TGG CGG GCT GTC TTC-**FAM**	81
DNA-target	GAA GAC AGC CCG CCA TAT CAA TGG AAA TCT CCC CAC ACA CAC ACA CAC ACA CAC AAT TCA TAG AGT CAT GAA ATT TTA TAG GTG GTC CCA CTC ATC CTC TGA	103
Primer Forward	GAA GAC AGC CCG CCA TAT CA	20
Primer Reverse	ATC AGA GGA TGA GTG GGA CC	20

SH - thiol group; **FAM** - fluorescein.

Table 2. Selected values for the electrochemical genosensor construction.

Variables	Tested range	Selected value
DNA Capture probe concentration (μM)	0.25–10.00	1.00
MCH concentration (μM)	0.00–1.00	1.00
MCH incubation time (min)	15–60	30
Homogeneous hybridization incubation time (min)	15–60	30
Temperature (ºC)	25-98	25
DNA-signaling concentration probe (μM)	0.13–0.50	0.25
Heterogeneous hybridization incubation time (min)	15–60	30
Antibody concentration (U/mL)	0.50–2.00	2.00
Antibody incubation time (min)	15–60	60

Table 3. Analytical parameters of the developed genosensor.

Parameters	Results
Linearity (nM)	0.03 – 1.00
Slope	1.53
Interception	0.04
Correlation (R)	0.992
Slopes' standard deviation	0.04
Interceptions' standard deviation	0.01
LOD	0.03
LOQ	0.10
Repeatability^{n} (%)	2.49
Reproducibility^{n} (%)	2.90
Total precision (%)	4.08

n = 5

Table 4. Portuguese honey bloom calendar [adapted from: 15].

Bloom	Jan	Fev	Mar	Apr	May	Jun	Jul	Agu	Set	Oct	Nov	Dez
Arbutus unedo												
Echium plantagineum												
Erica arborea												
Erica umbellate												
Castanea sativa												
Eucaliptus globulus												
Helianthus annuus												
Lavandula stoechas												
Citrus sinensis												
Quercus pyrenaica												

Table 5. Ct values obtained for the tested samples using three primer pairs targeting *Castanea sativa*.

Sample	*Castanea* (Ct)
Rs	28.43
H1	30.94
H3	27.26
H4	28.30
H5	26.79
H7	28.17
H11	27.95
Nc	34.41